CHALMERS
UNIVERSITY OF TECHNOLOGY

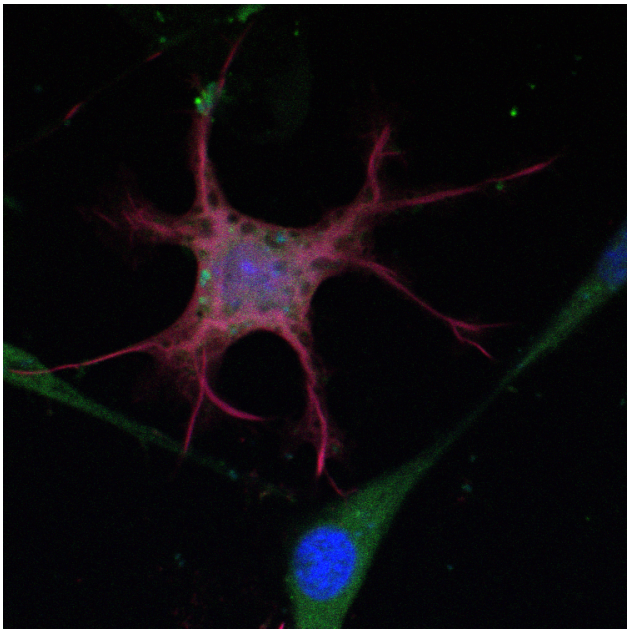

Mimicking embryonic interactions with engineered cell-culturing techniques

Using NIH3T3 murine embryonic fibroblasts to model compaction of the mammalian embryo

JAKOB OBERMÜLLER

Department of Biology and Biological Engineering
CHALMERS UNIVERSITY OF TECHNOLOGY
Gothenburg, Sweden 2017

Master's thesis 2017

Mimicking Embryonic Interactions with Engineered Cell-culturing Techniques

Using NIH3T3 murine embryonic fibroblasts to model compaction of the mammalian embryo

JAKOB OBERMÜLLER

Department of Biology and Biological Engineering
Division of Chemical Biology
Developmental Cell Dynamics Laboratory
Chalmers University of Technology
Gothenburg, Sweden 2017

Mimicking Embryonic Interactions with Engineered Cell-culturing Techniques
Using NIH3T3 murine embryonic fibroblasts to model compaction of the mammalian embryo
JAKOB OBERMÜLLER

Supervisor: Emanuele Celauro, Department of Biology and Biological Engineering
Examiner: Pernilla Wittung-Stafshede, Department of Biology and Biological Engineering

Master's Thesis 2017
Department of Biology and Biological Engineering
Division of Chemical Biology
Developmental Cell Dynamics Laboratory
Chalmers University of Technology
SE-412 96 Gothenburg
Telephone +46 31 772 1000

Cover: Fluorescence microscopy image of filopodia-expressing NIH3T3 murine embryonic fibroblast.

Typeset in LaTeX
Printed by [Name of printing company]
Gothenburg, Sweden 2017

Mimicking Embryonic Interactions with Engineered Cell-culturing Techniques
Using NIH3T3 murine embryonic fibroblasts to model compaction of the mammalian embryo
JAKOB OBERMÜLLER
Department of Chemical Biology
Chalmers University of Technology

Abstract

Compaction of the mouse embryo is triggered by the formation of filopodia by some of the blastomeres. These finger-like processes extend onto neighboring cells, providing mechanichal tension and possibly sending a signal that mediates compaction [1]. To investigate whether filopodia-mediated contact induces a transcriptional response in the receiving cells, NIH3T3 murine embryonic fibroblasts were used to design a model system for compaction. Two different cell-cultures were generated from the fibroblasts by inducing filopodia-formation in one culture (filopodia-expressing cells: FECs) and by adding a membrane marker to the other (non-expressing cells: NECs), allowing for separation on a column. These populations were to be co-cultured to allow filopodial contact to be established between them, after which the contact-receiving cells were to be isolated. The transcriptome of the filopodia-receiving cells would then be characterized. Induction of filopodia could not be achieved by transfecting the fibroblasts with *Egfp-Myo10* a method used by Fierro-Gonzaléz *et al.* [1]. However, transfection of *Gfp-Cfl1*-constructs encoding GFP-cofilin resulted in filopodia-formation. This provided a reliable method to generate FECs from the fibroblasts. Moreover, an NEC cell-line that stably expressed the membrane tag *Vamp2-Sbp* was generated using antibiotic resistance on the *Vamp2-Sbp* plasmid. Collectively, these results show that the underlying mechanisms behind filopodia-formation may vary, depending on cell-type and environmental parameters such as substrate composition. Furthermore, the findings provide a firm base upon which to build a model system to further study the intercellular filopodial contact in mammalian cells.

Keywords: compaction, filopodia, embryo, fibroblasts.

Acknowledgements

I would like to thank Juan Carlos Fierro-González for giving me the opportunity to be a part of his team for my thesis project, as well as his help with the editing of this thesis. At the time of writing he has recently become a father, and I wish him and his family a happy life and a bright future. I would also like to thank Pernilla Wittung-Stafshede for being my examiner. A big thanks to everyone at the office in MC2 at Chalmers for being so welcoming, and providing me with a pleasant working-environment and weekly fika. The one other person beside myself most involved with this thesis project is my supervisor Emanuele Celauro. Thank you Emanuele for tirelessly helping me and supporting me through this project. You have not only been an excellent teacher and mentor, but I have had much fun working with you. I wish you all the best in everything you set out to do. Finally, I want to thank the friends I have made at Chalmers during my years of studying here, as well as my family.

Jakob Obermüller, Gothenburg, May 2017

Contents

1

Introduction

Compaction is an event that occurs at the 8-cell stage of mammalian embryonic development[2, 3, 1, 4]. During compaction, intercellular tension forces result in cell elongation, and as a result the previously spherical embryo cells form a more compact mass of cells [1, 3]. Compaction is also the first of a series of morphological changes, including apicobasal polarization, that eventually lead to the divergence of the first dedicated cell lineages; the initially homogeneously pluripotent cell population of the pre-compaction embryo (these initial cells are known as blastomeres) emerge afterwards as two distinct cell-types [5, 6, 7, 4]. The embryonic core consists of the inner cell mass (ICM), surrounded by the trophectoderm (TE) [7, 8]. The ICM will later form the embryo proper and remains pluripotent, whereas the TE will form the extraembryonic tissues, including the placenta [7, 8]. Pluripotency is a property related to expression of octamer binding transcription factor 4 (*Oct4*). ICM cells that do not express *Oct4* lose pluripotency and commit to TE lineage [9]. TE cells are by contrast characterized by expression of caudal type homeobox 2 (*Cdx2*), which is not expressed at all in ICM cells [9]. *Cdx2* has been demonstrated to inhibit *Oct4* expression in TE, and *Cdx2* null-mutant mouse embryos die between 3.5-5.5 days postcoitum, starting around the formation of the TE and the first point of *Cdx2*-expression[9, 10].

Although it is known that compaction is essential to make viable embryos, much of the process is still not understood [11, 3, 1]. Fierro-González *et al.* [1] found that approximately half of the blastomeres at the 8-cell stage form filopodia during compaction. These filopodia were shown to be important for maintaining the tension forces that drive compaction. Filopodia are finger-like protrusions of the cell membrane that are involved in cell sensing, motility and cell-cell contact [12, 13, 2]. They consist of tighly packed parallel actin filaments, stretching from the base to the tip of the filopodium [12, 13, 2]. During compaction, filopodia extend from the interface between two blastomeres onto the membrane of a neighboring cell (see figure 2.4). They found that inducing early filopodia formation in some blastomeres by overexpressing *Myo10* triggers early compaction. Furthermore, inhibiting filopodia formation by knockdown of filopodia components E-cadherin, α- and β-catenin, F-actin and myosin-X disrupted filopodia formation and prevented the affected cells from integrating into the compacted embryo.

Filopodia thus appear to mediate the transmission of some physical or chemical signal that induces compaction in the filopodia-receiving cells. Although these findings help unveil some of the biomechanics involved in embryo compaction, it still remains unknown how this signal is relayed. It is possible that the attachment and mechanical tension provided by the filopodia induces compaction in the receiving

cells. Adhesion receptors, acting as connectors between the cytoskeleton and surrounding environment, are known to translate extracellular tensions into signalling pathways that generate a cellular response [14]. Perhaps, the tension provided by the filopodia does not itself trigger compaction, and instead it is increased cell-cell contact area between neighboring blastomeres as a result of filopodia-mediated tension [1] that allows for a higher flux of signalling molecules across the membranes between the cells. It is also possible that the filopodia actively transport signalling molecules between the filopodia-extending- and receiving cells. In chick embryos, non-neighboring cells communicate by forming long filopodia that may traverse several intermediate cells to transport signalling molecules between them, using the filopodia as conduits [15].

As compaction is a rather drastic event, both in terms of the morphological transformation of the cells and their subsequent differentiation, it seems likely to be accompanied by a change in the transcriptional profile of the cells. Some set of genes responsible for maintaining the pre-compaction phenotype are presumably down-regulated and some other set of genes are presumably activated to drive on the metamorphosis into the post-compaction phenotype. Since compaction of the embryo immediately precedes the very first cell differentiation event [5, 6, 7, 4], it is possible that the filopodia-mediated signal regulates genes involved with determining the pluripotent state of embryonic stem cells, including *Oct4* and *Cdx2*, although findings made by Fierro-González *et al.* suggest that there is no correlation between a blastomere forming- or receiving filopodia during compaction and its subsequent lineage commitment. It is also possible that the filopodial contact controls the order in which the compacting cells undergo division, perhaps by regulating genes involved in cell-cycle progression, such as the cyclin dependent kinase (*Cdk*) gene family [16]. Another possibility still is that the filopodial signal induces a re-arrangement of the actin cytoskeleton in the signal receiving cells, or an increase in cell-cell adhesion molecules. This could help provide the intercellular tensions that occur during compaction [1, 3]. Such a response would be characterized by a change in the transcriptional levels of actin-regulating genes such as myosins [17, 18, 19], cofilin [20, 21] or cell-adhesion molecules such as members of the cadherin superfamily [22].

The aim of this master's thesis project was to develop a model system that could be used to study signalling driven by filopodia during compaction of the embryo. While it is certainly possible to do this in actual embryos, a simpler model system could be made easier to manipulate and monitor as well, and could allow for a higher throughput of experiments and generation of data. Selected findings of particular interest could then be studied in actual mouse embryos for validation. NIH3T3 murine embryonic fibroblasts were chosen as the model cells because of their relative proximity to embryonic blastomeres from a developmental standpoint, for their known ability to form filopodia [23], and because they are a commonly used cell line with an abundance of available protocols for experimental procedure.

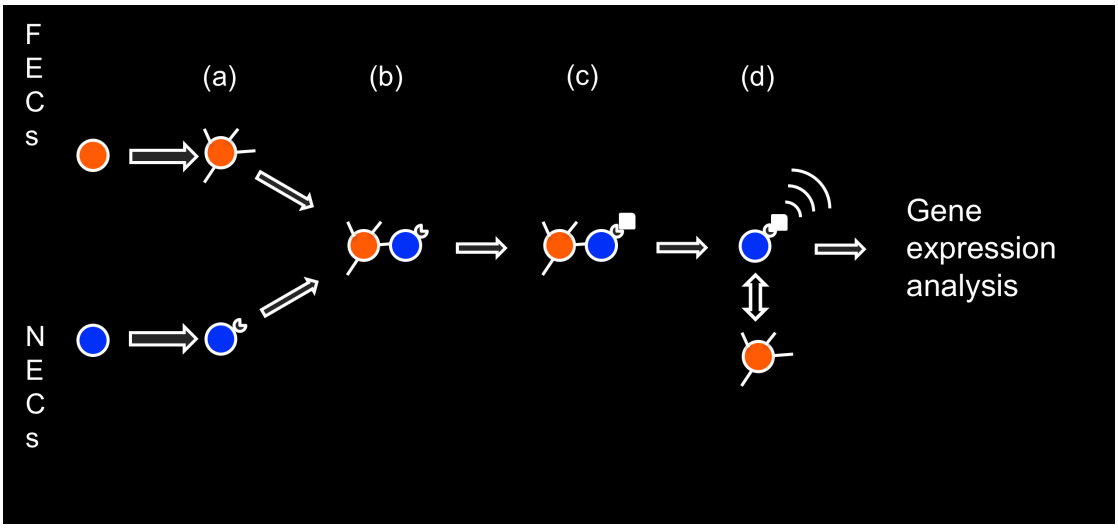

Figure 1.1: Schematic overview of the project plan: (a) in the first phase of the project, filopodia-formation is induced to obtain the filopodia-expressing cells (FECs) by overexpression of a transfected gene. Different genes were to be tried to identify one that worked. Meanwhile, a membrane marker is added to the non-expressing cells (NECs) by transfecting them with a palmitoylation/myristoylation signal from the Lyn kinase gene [24] that is not present in the FECs. To inhibit undesired filopodia-formation by the NECs, they would either be transfected with a filopodia-inhibiting gene, or filopodia-formation would be blocked using antibodies (b) In the second phase, the FECs and NECs are co-cultured to allow the FECs to make filopodial contact with the NECs. (c),(d) After an established filopodial contact, the tag on the NECs would be used to separate the sub-cultures and isolate the NECs to characterize their transcriptional profile.

The plan was to make a co-culture consisting of equal parts of filopodia-expressing cells (FECs) and non-expressing cells (NECs) that did not form filopodia. The filopodia of the FECs would make contact with NECs, likely producing some measurable reaction in the transcriptome of the NECs. After this contact had been established, the cells would be separated using a membrane marker in the form of a palmitoylation/myristoylation signal from the Lyn kinase gene [24] on the NECs, and a transcriptional profile of the NECs would be analyzed and characterized using reverse transcription real-time quantitative polymerase chain reaction (RT-qPCR) [25]. Working under a hypothesis presented by Fierro-González et al. that the filopodia-mediated compaction signal is unrelated to the future transcriptional state of the signal-receiving cells [1], focus was initially to be on genes involved with maintaining pluripotency (*Oct4* [26], *Cdx2* [9], Sox2 [27], *Nanog* [28] and *Eomes* [29]), to confirm their findings, and then on genes involved in cell-cycle regulation (Cdk's [16]) and actin regulation (myosins [17], cofilin [20] and cadherins [22]).

Parallel experiments, carried out by postdoctoral researcher Emanuele Celauro, at our department of biology and biological engineering at Chalmers University of Technology, would generate a corresponding transcriptional profile of the NECs of actual mouse embryos. The transcriptomes from the model system and the actual embryos would be compared for similarity, answering whether there is a general ge-

netic response for filopodia-mediated contact that is conserved between blastomeres and embryonic fibroblasts and whether the NIH3T3 model system can be used to study the role of filopodia in compaction of the mammalian embryo.

Because of the time-constraint of my 6-month thesis project, it was decided that I would join the project during my allotted time-frame, after which I would report on the progress thus far.

2

Theoretical background

2.1 Filopodia

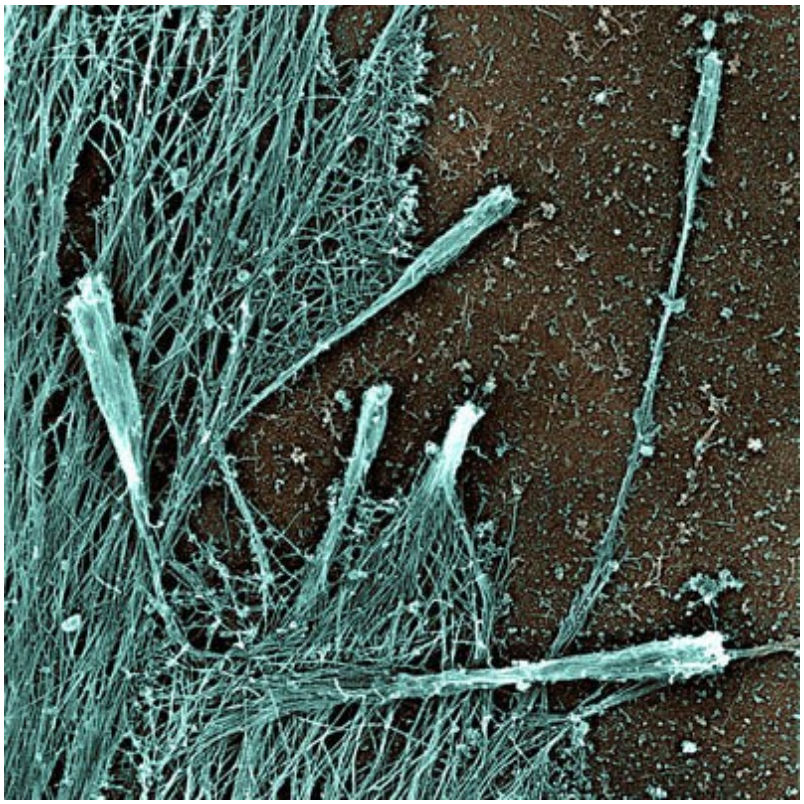

Figure 2.1: Colorized SEM-micrograph of filopodia extending from a cultured cell. This image was reprinted under a Creative Commons Attribution 2.5 Generic License `https://creativecommons.org/Licenses/by/2.5/`. The original image can be found in [30]

.

Filopodia are actin-rich, slender protrusions of the cellular membrane [12, 13, 2]. They can be found in various cell types, and are involved in several different cellular activities. They were first discovered in migrating mesenchymal cells of the sea urchin embryo, appearing as small bristles located at the front of the cell along the axis of movement [31]. The filopodia were rapidly extending and retracting, as well as flailing about in sweeping motions. The location and behavior of the antennae-

like organs indicated that they probed the environment for spatial information that could guide the movement of the cells.

This role in which filopodia was first observed is typical. Filopodia are often found growing upon larger, sheet-like, actin-rich protrusions of the membrane called lamellipodia [13, 2]. In the case of cell migration, the cell extends a large lamellipodium in the direction of movement, with filopodia extending from the leading edge like fingers from a hand. Both these structures form adhesion points with the substrate and allow for the cell to drag itself forward [2]. The functional analogy between filopodia and human digits holds true insofar as both have sensory as well as gripping roles [13, 2]. Since their discovery, filopodia have been associated with many different cell functions in addition to cell migration and adhesion, including chemotaxis, extension of the neural growth-cone and embryonic development [13, 2]. Having excessive filopodial activity is also a characteristic of invasive cancer cells [13]

Filopodia are supported internally by tightly packed bundles of parallel actin filaments that run the entire length of the structures, from base to tip. This is in contrast to the larger lamellipodia, that instead consist of a dense meshwork of actin [13, 2, 12]. Filopodia formation is initiated by the nucleation of a protein complex in very close proximity to the intracellular face of the membrane [32]. This complex then serves as a starting site where actin assembles into a bundle of short filaments pointing in the direction of extension, to serve as the base of the filopodium. More actin then continues to polymerize at the tips of the filaments, called the "barbed ends", causing the entire membrane to protrude around it as it extends. The actin polymerization often happens at a faster pace than the membrane protrusion, causing the actin filaments to slide backwards into the cell as they grow. This constant retrograde flow of the actin filaments help make the filopodia dynamic, since filopodia length can be regulated by adjusting the rate of polymerization[32]. A filopodium in mammalian embryos, for example, can extend or retract in less than an hours time [1]. The internal molecular machinery involved in filopodia regulation is complex and includes many different proteins and factors. A schematic of filopodia, including the inner workings of the structure, can be found in figure 2.2. [2]

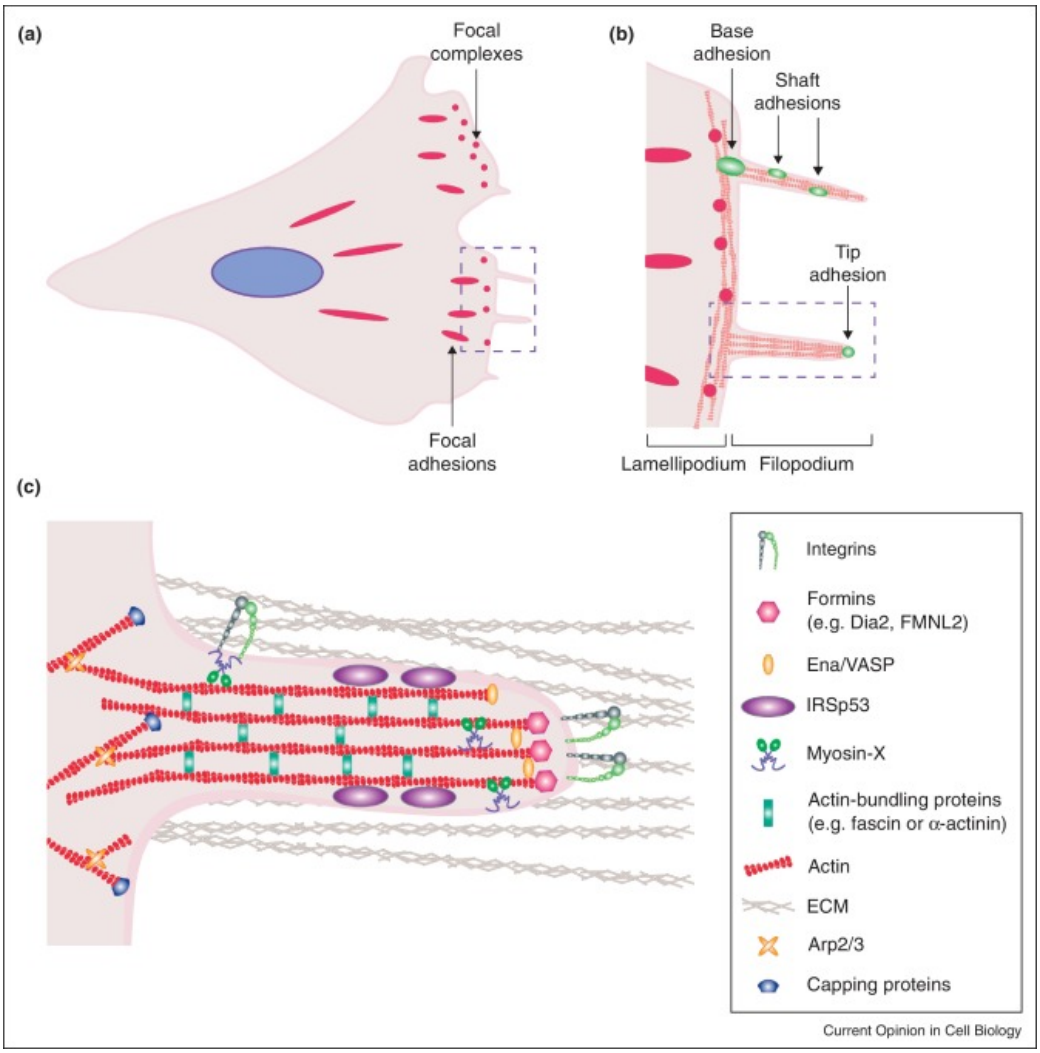

Figure 2.2: Schematic over filopodia during migration of a cell across a 2D-substrate. (a) Filopodia, stretching from lamellopodia located at the leading edge of the cell, find adhesion points on the substrate to allow for further migration along the axis of movement. (b) Different adhesion complexes located at various locations of the filopodia allow the filopodia to connect the substrate to the actin framework that stretches the filopodia. (c) A more detailed schematic of the molecular composition of the filopodia. The bulk of a filopodium consists of parallel actin filaments oriented along the long axis of the structure, held together by crosslinking proteins such as fascin. Insulin-receptor substrate p53 (IRSp53) deforms the cellular membrane, facilitating the formation of filopodia. F-actin extension at the tip of the filopodium is mediated by myosin X motor proteins, which carry important proteins and other factors along the actin fibers to the tip region. Such factors include adhesion molecules such as integrins and cadherins. Reprinted under the Creative Commons Attribution-NoDerivatives 4.0 International License `https://creativecommons.org/Licenses/by-nd/4.0/`. The original image can be found in [33]. The figure is unchanged, apart from the caption, which has been rewritten.

2.2 Compaction of the mammalian embryo

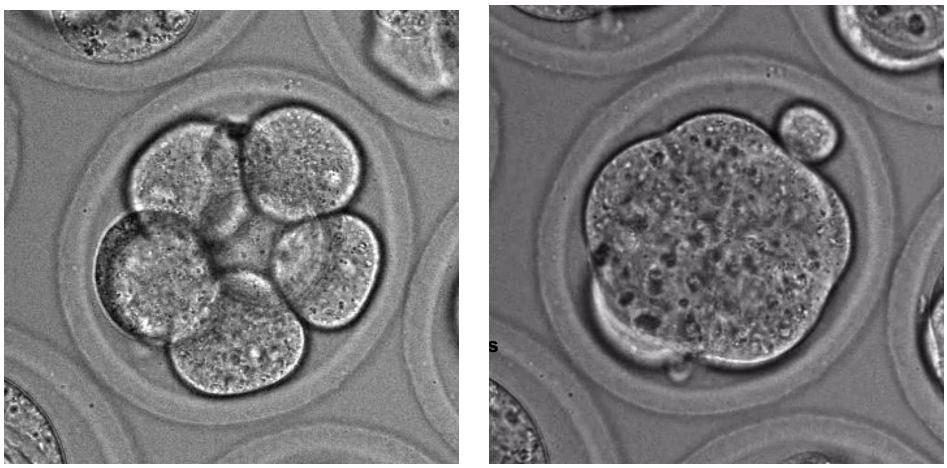

(a) **(b)**

Figure 2.3: *In vitro* fertilized mouse embryo before and after 8-cell stage compaction. the cells are enveloped in the protective *zona pellucida* (a) Uncompacted embryo. The cells are spherical and easily distinguished due to their clear intercellular borders (b) Compacted embryo. After compaction, the embryo appears as a single mass, and it is now difficult to count the constituent cells. At a glance, the wavy border region of the embryo is perhaps the only clue that it does in fact consist of several individual cells. Reprinted with permission. Fierro-González, unpublished results.

Mammalian embryonic development starts after a cell-stage arrested ovulated egg is fertilized by a single sperm, merging the two gametes into a single celled embryo called a zygote [4]. 16-20 hours later, the single cell divides into two cells [4]. These early embryonic cells are called blastomeres, and are characterized by their spherical shape, lack of polarity, totipotency and lack of general function save for the preparation of their next division. The blastomeres keep dividing until the embryo consists of 8-16 cells and then begins the first major morphological change of the constituent cells since fertilization, namely compaction [7].

Compaction is a term used to describe a maximization of adhesive contact between cells, driven by an increase of intercellular adhesion molecules such as cadherins [34]. Tissue compaction can be observed several times during vertebrate embryonic development [35], in cultured tissues [36] as well as in post-embryonic tissues, for example during wound healing [34]. On the cellular scale, compaction of the mammalian embryo is characterized by increased cell-cell contact as neighboring cells flatten their membranes at the interface, similar to how two balls pressed together would increase their contact area if deflated. Compaction is a critical process to the tissues that undergo the event, and failure to compact is generally associated with a loss of viability in those tissues [35]. For example, human embryos that have been fertilized *in vitro* are rendered non-viable in case of failed compaction. [35, 1]

As the mammalian embryo compacts, a characteristic change in the embryonic morphology can be seen. The embryo transforms from appearing as a cluster of loosely associated cells to contracting into a single spherical mass, where the individual cells are less distinguishable [1]. The post-compaction embryo is called a *morula* [35], the latin name for the mulberry which it supposedly resembles. The cells of the morula are now polarized, with an apical domain facing the outside of the embryo and basolateral domain facing the neighboring cells. This polarity is also reflected in the differing populations of membrane-associated proteins between the two domains. The apical membrane protein ezrin exclusively associates with the apical domain, whereas PAR polarity protein Par3 is restricted to the basolateral domain [7]. The borders that separate the apical- and basolateral regions of the morula are rich in adherens juctions [7, 8, 1].

When the cells of the morula start to divide, they can do so symmetrically or asymmetrically. Symmetric division occurs when both daughter cells locate to the embryonic surface. In the case of asymmetric division, one daughter cell instead locates toward the center of the embryo, becoming completely surrounded by other cells. [35, 37, 1]. Asymmetrical division was proposed to be the leading cause for blastomere internalization in the early morula, but recently a second mechanism has been suggested. As the polarized blastomeres of the morula divide, the daughter cells inherit unequal amounts of apical material, such as the essential apical protein aPKC [38]. This results in the 16-cell embryo consisting of both polarized and unpolarized cells. The unpolarized blastomeres have a higher actomyosin contractility than their polarized neighbors, causing them to migrate into the center of the embryonic mass [39]. Maître *et al.* proposed a cause for the differential contractility of the blastomeres, where aPKC antagonizes myosin in the apical domain. The asymmetric inheritance of aPKC between daughter cells causes the unpolarized cells to express myosin even in their outward-facing region, increasing actomyosin contractility and causing internalization [40].

The internalization of some blastomeres establishes two different cell types, not only in terms of location within the embryo, but also in terms of gene expression and cell-lineage dedication [1]. Compaction of the embryo thus immediately precedes the first differentiation event [7]. Where all the blastomeres of the pre-compaction embryo are functionally and transcriptionally identical, the late morula consists of an inner cell mass (ICM) of pluripotent non-polar cells enveloped in a layer of differentiated polarized epithelial cells, called the trophectoderm (TE) [7]. The inner mass will later form the embryo proper, and the trophectoderm will give rise to the extra-embryonic tissues. [11, 41].

2.3 A previous project by Fierro-González *et al.* forms the basis for this thesis

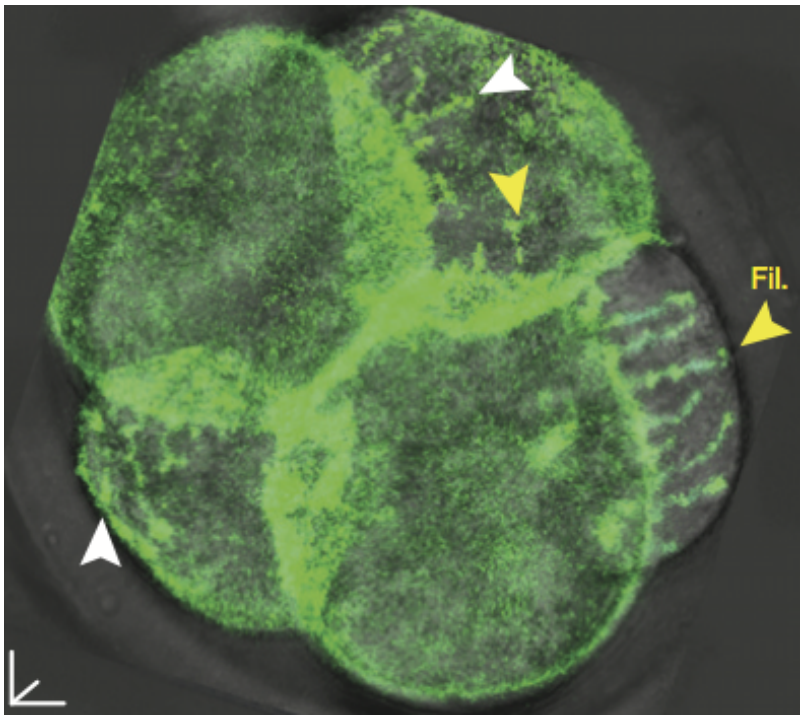

Figure 2.4: Mouse 8-cell embryo at the early stages of compaction. Microinjection of GFP-tagged E-cadherin was injected at the 2-cell stage, which revealed the formation of filopodia by ca. 61% of the embryonic blastomeres. The filopodia formed at the intercellular borders and extended onto neighboring cells. Reprinted with permission. The original image can be found in [1].

This thesis project builds largely on the findings presented by Fierro-Gonzaléz *et al.* [1]. Their project aimed to characterize compaction of the mouse embryo further by finding the cause of the event. They reasoned that compaction likely depends on cell-cell interactions between the blastomeres, since the early embryo is encapsulated by a protective envelope, called the *zona pellucida*, and therefore has no direct contact with the surrounding environment. By inhibiting E-cadherin - an adhesion molecule involved in many cell-cell interactions - with antibodies, they could induce compaction defects in the embryos. Deleting the gene *Cdh1* that codes for E-cadherin had the same effect. Microinjecting *Cdh1* fused with *Gfp* in one of the blastomeres at the 2-cell stage led to the identification of filopodia that form at the 8-cell stage just before compaction.

Their findings showed that compaction of the mouse embryo is initiated when some of the blastomeres form filopodia that extend onto the neighboring cells. During this event, roughly 61% of the blastomeres formed filopodia, and two cells never extended filopodia reciprocally onto each other. This allowed categorization of the blastomeres as either being filopodia-extending cells (FECs), or non-extending cells

(NECs). Furthermore, the filopodia first formed during the 8-cell stage and were absent again during the 16- to 32-cell stages after completed compaction. Each FEC formed on average 5.6 filopodia per neighboing cell, and extended them onto an average of 2.4 neighboring cells. The filopodia extended during 303 ± 46 min and then retracted again over 60 ± 9 min.

The filopodia-forming event was found to correlate with cell division events. FECs never divided while extending filopodia, and always underwent cell division after retracting their filopodia. Furthermore, NECs never underwent cell division while receiving filopodial contact. These findings suggest that filopodia formation may control the order in which the cells divide, possibly to maintain the structural integrity of the embryo. The FECs had a visible change in the shape of their apical membranes as a result of filopodia formation. The membranes were flattened, as if they were stretched like drum skins as the cells pulled on their neighbors. Severing the filopodia with lasers caused the membrane to relax to a higher curvature as the cells reverted to more spherical form, affirming that the filopodia provided mechanical tension.

Moreover, 69% of FECs underwent symmetric division, where both daughters allocated to the outer embryonic regions that later form the trophectoderm, and the remaining 31% underwent asymmetric division, where one daughter cell allocated to the embryonic center that later forms the inner cell mass. This ratio between symmetric and asymmetric divisions has been previously observed in compacting embryos, suggesting no apparent correlation between FEC/NEC status and cell lineage commitment.

2.4 *Vamp2-Sbp*

VAMP2, or Vesicle-Associated Membrane Protein 2, is part of a protein complex involved in the membrane-fusion of neurotransmitter-containing synaptic vesicles in the human brain. More specifically, the protein is believed to mediate neurotransmitter-release at a certain step between vesicle docking and fusion. VAMP2 is a transmembrane protein, consisting of a cytoplasmic-, transmembrane- and extracellular region. [42]

No functional association between VAMP2 and F-actin or filopodia formation has been described by the scientific literature at the time of writing this thesis, and use of the human ortholog of the protein could further reduce the risk of VAMP2 interfering with any pathways directly involved in filopodia-formation in mouse cells. The role of VAMP2 in this project was to serve as a non-invasive membrane marker and anchor for isolation of cells transfected with the protein. For this reason, the region of the gene coding for the extracellular domain of VAMP2 was truncated and replaced with streptavidin-binding peptide (*SBP*).

SBP is a streptavidin-binding peptide sequence that can be used for detection and purification of SBP-containing recombinant proteins. The sequence is 38 amino acids long and has been shown to yield more pure samples than those using comparable purification-tags such as the hexahistidine tag. SBP is a nanomolar-affinity tag, binding tightly to streptavidin. Even so, elution conditions are mild, and SBP can be dissociated from streptavidin by treatment with biotin dissolved in a wash

buffer. [43]

2.5 *Myo10*, myosin-X

Myosin-X, or MYO10, belongs to the myosin superfamily of motor proteins [17, 18]. Myosins transport other molecules around the cell by carrying their cargo while moving along actin filaments (F-actin). Myosins consist of two functional regions. The motor region provides movement along actin by a proposed walking mechanism, and the tail region is linked to the cargo [18].

To harvest the energy required for locomotion, myosins hydrolyze ATP continuously [17, 18]. Myosin-X - like most myosins - moves toward the plus-end of actin filaments, meaning it migrates along the direction of polymerization, away from the filament base and towards the barbed end [17]. In the case of filopodia, recycling of myosin-X, moving the protein back from the tip region toward the cell body, is likely a passive process where the protein simply halts its motor function and rides the retrograde flow of the filaments back to the base region [19].

Myosin-X has been implicated as a central actor in the formation of filopodia [1, 19, 44]. GFP-fused myosin-X localizes and accumulates at the tips of filopodia, which is also the location of actin filament barbed ends [44]. Since this is the region where actin polymerizes to extend the filopodia, it is presumably a region where filopodia extension and retraction is regulated. Furthermore, overexpression of full-length myosin-X has been shown to increase the number and length of filopodia in various cell types, among them NIH3T3 fibroblasts [19, 1, 44]. It is not understood exactly what role myosin-X plays in the formation of filopodia, but suggestion include transporting other essential filopodial components, such as integrins and ENA/VASP-proteins to the polymerizing tip region, as such components co-localize with myosin-X as it migrates along the filopodia [13]. While transportation of essential components certainly may be one of the roles of myosin-X in the filopodial machinery, there are experimental results that suggest a more complex function. Truncated myosin-X that lacks a tail region is sufficient for initiating filopodia-formation, but results in short and unstable filopodia [44]. This indicated that the motor-function of myosin-X is required for initiating filopodia-formation, and the tail region is required for continued elongation, structural integrity and stability of the filopodia [44, 2].

2.6 *Cfl1*, cofilin

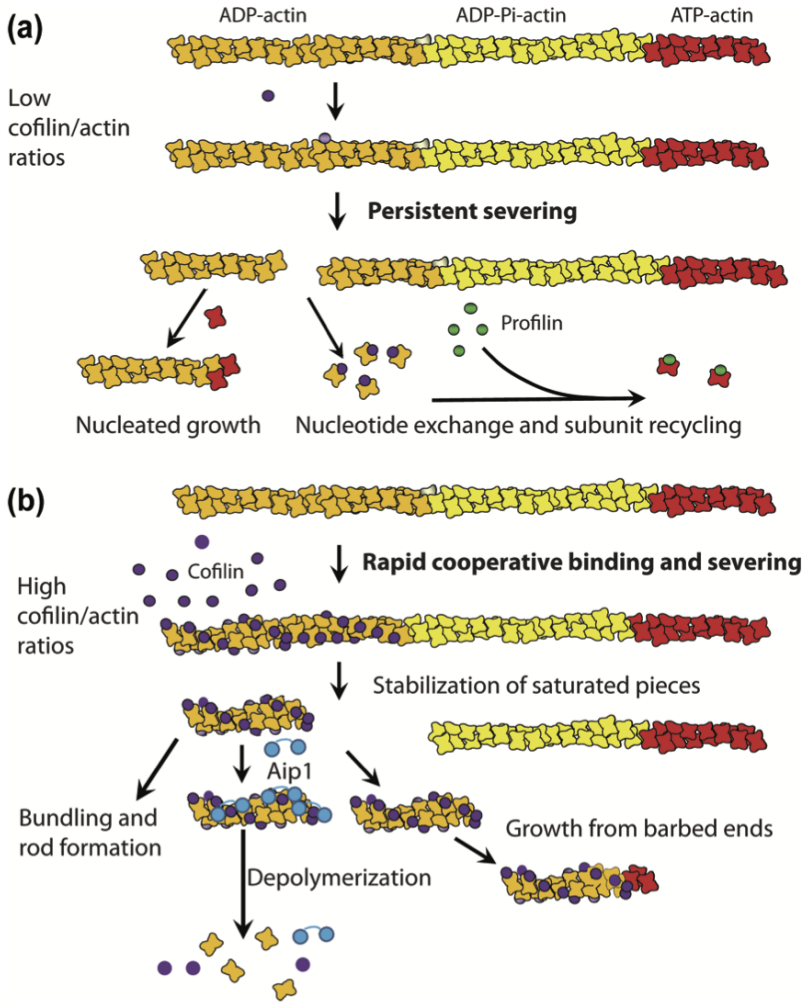

Figure 2.5: Schematic over two different effects of cofilin acting on F-actin. (a) shows how a low ratio of cofilin/F-actin promotes F-actin disassembly. (b) shows how a high ratio of cofilin/F-actin converts regular F-actin into cofilin-stabilized "rods" of bundled filament fragments. This figure is reprinted under the Creative Commons Attribution-NonCommercial License (`http://creativecommons.org/Licenses/by-nc/3.0/legalcode`). The original image is found in [21]

Cofilin is encoded by the *Cfl1* gene and is a protein involved in regulating the dynamics of actin polymerization and depolymerization [20, 21]. All eukaryotes express one or more member of the actin-depolymerization factor (ADF)/cofilin family. Cofilin acts by binding to ADP subunits in filamentous actin, severing the filaments and thus maintaining F-actin dynamics. The result of cofilin acting upon F-actin depends on the molar ratio of cofilin to the actin subunits in the filaments. At low ratios, where the cofilin concentration is lower than 1% of the actin subunit concentration, persistent severing of the actin filament occurs, splitting it into multiple shorter filaments. The cofilin-bound subunits that were located at the

break point are recycled, and repolymerization occurs at the newly created barbed end.

If instead cofilin is present at a higher molar ratio, with a concentration that exceeds 10% relative to that of the actin subunits, the outcome changes drastically. Instead of severing the filaments into oligomeric units that dissociate, the filaments become saturated with cofilin units that form stabilized complexes with the ADP-actin. The filaments are still severed internally but instead of dissociating completely, the cofilin-covered fragments bind each other and bundle together in a twisted form. These aggregates of twisted filament fragments are called rods, and can generally be reversed by the cells into regular actin filaments. Other proteins involved in actin assembly and disassembly - such as actin-interacting protein 1 (AIP1) or tropomyosins, to name a few - may affect the effect cofilin has on F-actin regulation. This may partly be due to competitive inhibition by these different components of the regulatory machinery binding to F-actin. [21]

3

Materials and Methods

3.1 Cell Preparation and Maintenance

NIH3T3 Murine fibroblasts, ordered from ATCC (Catalog # CRL-1658) were thawed from storage in liquid nitrogen and cultured in a T25 cell culture treated flask (Catalog #: 156367) from Thermo Scientific. The cells were then passaged every few days when the confluency reached 70-80%. The cells were passaged until at least passage number 10 before undergoing transfection. The cells were cultured in a 9:1 mixture of Gibco high glucose DMEM media ordered from Thermo Scientific (Catalog #: 41965039) and iron fortified Bovine Calf Serum (BCS) from ATCC (Catalog #: 30-2030), at 37 °C and 5% CO_2.

3.2 Plasmid preparation

pCS2-EGFP-MYOX plasmid was previously described by Fierro-González *et al.* [1]. pCS2-GFP-Cofilin plasmids were a gift from the Plactha lab, Institute of Molecular and cell Biology, Singapore. pcDNA3.1(+)-VAMP2-SBP plasmids were ordered from `www.addgene.org`. Schematics of the three plasmids are included in Appendix A. The plasmids were amplified in Invitrogen TOP10 chemically competent *E. coli*, ordered from Thermo Scientific (Catalog #: C404010), after which a midiprep was performed to recover the plasmids using a PureLink HiPure Plasmid DNA Purification Kit from Invitrogen, Thermo Scientific (Catalog #: K210004) following the manufacturer's instructions.

3.3 Plasmid linearization

The circular plasmids were linearized using restriction enzymes that did not interfere with the gene of interest or their promoter regions. The restriction enzyme ScaI from Thermo Scientific (Catalog #: ER0431) was used to linearize the pcDNA3.1(+)-VAMP2-SBP plasmid, and the restriction enzyme NdeI from Thermo Scientific (Catalog #: ER0581) was used for the pCS2-EGFP-MYOX and pCS2-GFP-Cofilin plasmids. The restriction digestions followed the manufacturer's instructions. The QIAquick Nucleotide Removal Kit from Qiagen (Catalog #: 28304) was used following the manufacturer's instructions to purify linearization products. Gel electrophoresis was performed to verify the expected plasmid lengths, and the

linearization products of pCS2-EGFP-MYOX and pcDNA3.1(+)-VAMP2-SBPwere used for mRNA synthesis.

3.4 Introducing Kozac sequence and SP6 promoter before *Vamp2-Sbp*

Kozac sequence and SP6 promoter were introduced before the *Vamp2-Sbp* fusion gene on an overhanging forward primer in a PCR-reaction to allow for mammalian cell expression and mRNA-synthesis using the mMessage mMachine SP6 kit from Thermo Fisher (Catalog #: AM1340), respectively. PCR was performed with Phusion Green Hot Start II High-Fidelity Polymerase ordered from Thermo Scientific (Catalog #: F537S), following the manufacturer's instructions, in a Techne PrimeG machine. The PCR program is described in table 3.1.

Table 3.1: PCR program used to introduce the SP6 promoter and Kozac region before *Vamp2-Sbp*

Cycle step	Temperature(°C)	Time	Cycles
Initial denaturation	98	30 seconds	1
Denaturation Annealing Extension	98 66.3 72	10 seconds 10 seconds 13 seconds	45
Final extension	72	10 minutes	1
Hold	4	Indefinitely	

The forward and reverse primer sequences are presented in table 3.2. They were custom-designed and ordered from Thermo Scientific using their "Value Oligos" synthesis service for non-modified, 25 nmole 5-40 mers DNA oligonucleotides. The primers were designed starting from the target sequences, and then trimmed to the correct lengths by calculating the melting temperatures for a Phusion polymerase using the T_m-calculator [45] from Thermo Scientific, and by avoiding hairpin structures using the Oligonucleotide Properties Calculator [46] from Northwestern University. The concentration and purity of the amplicon was measured in a NanoDrop 1000 spectrophotometer from Thermo Scientific, and then used for mRNA synthesis.

Table 3.2: Primer sequences used to introduce the SP6- and Kozac sequences before *Vamp2-Sbp*. The blue sections are overhangs containing the sequences to be introduced, and the red sections are annealing.

Primer	Sequence
(SP6/Koz/*Vamp2*)	5'ATTTAGGTGACACTATAGGCCGCCACCATGTCG3'
(REV/PolyA)	5'CCAGCTGGTTCTTTCCGC3'

3.5 mRNA synthesis

The mMessage mMachine SP6 kit from Thermo Scientific (Catalog #: AM1340) was used to produce mRNA using linearized pCS2-EGFP-MYOX and pcDNA3.1(+)-VAMP2-SBP plasmids as template. The synthesis followed the manufacturer's instructions. After the transcription reaction, the RNeasy Mini Kit from Qiagen (Catalog #: 74134) was used for mRNA purification, following the manufacturer's instructions. The concentration and quality of the resulting mRNA was measured using the NanoDrop 1000 spectrophotometer from Thermo Scientific, and the mRNA was then stored at $-20\,^{\circ}\mathrm{C}$. Before freezing, small volumes were aliquoted before storage to avoid degradation due to re-thawing and re-freezing.

3.6 Coverslip treatments

Borosilicate no. 1 coverslips from Corning (Catalog #: 2845-18) were initially coated using poly-D-lysine from Life Technologies [1]. After finding that polylysine coats may not allow filopodia adhesion due to the lack of integrin adhesion sites, an alternative method of coating the coverslips using Geltrex LDEV-free Reduced Growth Factor Basement Membrane Matrix from Thermo Scientific (Catalog #: A1413201) was used. Geltrex-coating was performed following the "thin gel" method described by the manufacturer and UV-sterilized overnight, or used as a 1:1 (v/v) mix with complete growth medium.

3.7 Cell transfection

NIH3T3 cells were detached from the flat bottomed culture flasks and seeded in Corning 12-well plates, ordered from Sigma-Aldrich (Catalog #: SIAL0513-50EA), containing one treated coverslip per well. The cells were allowed to attach properly before being transfected with either plasmids or mRNA. For mRNA-transfection, the Lipofectamine MessengerMAX reagent from Thermo Scientific (Catalog #: LMRNA003) was used, and for plasmid-transfection, the Lipofectamine LTX with PLUS reagent from Thermo Scientific (Catalog #: 15338100) was used. Both transfection methods followed the manufacturer's instructions. On the 12-well plates, the wells of each column had varying amounts of genetic material (plasmid DNA or mRNA) and the wells of each row had varying amounts of transfection reagent. This way, each well contained a unique combination of genetic material and transfection reagent. One mock-column was always included, where the cells were treated with transfection reagent but without mRNA or plasmid. This was to identify any adverse effects the reagent may have had on the cells. The transfected cells were incubated at $37\,^{\circ}\mathrm{C}$, 5% CO_2 for 16 or 24 hours to investigate if there was a difference in gene expression levels over time.

[1] Life Technologies was acquired by Thermo Fisher Scientific in 2014.

3.8 Inhibiting filopodia formation with α-cadherin antibodies

Cells were trypsinized and diluted to have 4 x 10^4 cells per well at day zero in a tissue-culture treated 12-well plate. The next day, a range of different amounts of anti-Cdh1 antibody (raised in rat) were added directly to the growth medium, to get the following dilutions: 1:200, 1:400, 1:800 and 1:1600. A well was always kept as a negative control, without adding any antibody. Cells were then incubated for 24 hours, before undergoing standard fixation. To determine the effect of anti-Cdh1 on filopodia formation, fixed cells were incubated for 1h at room temperature with anti-MYO10 (raised in mouse) and counterstaining was performed using phalloidin conjugated with AlexaFluor-488 or -568, to stain F-actin, and DAPI for the nuclei.

3.9 Generating a stable cell line using G418 geneticin

A stock solution of 50 mg ml^{-1} active G418 from Sigma-Aldrich (Catalog #: 108321-42-2) was prepared following the manufacturers protocol, by adding a 1 g G418 vial to 3.55 ml PBS. The drug was sterile filtered using a syringe and a 0.2 µm filter and then stored at 4 °C until used.

NIH3T3-cells that had been transfected with the pcDNA3.1(+)-VAMP2-SBP plasmid, containing geneticin-resistance, were transferred to polylysinated coverslips placed into wells on a 12-well plate. Each well contained DMEM/BCS-medium with increasing fractions of G418, ranging from 24 µg to 25 mg. A mock dilution, which contained no geneticin, was included as a control.

Table 3.3: Dilution series of geneticin, starting from a 50 mg ml^{-1} initial concentration of geneticin in PBS. The geneticin solution was diluted in DMEM.

Dilution factor	Conc. (µg ml^{-1})
1:2	25,000
1:4	12,500
1:8	6,250
1:16	3,125
1:32	1,527
1:64	781
1:128	391
1:256	195
1:512	98
1:1024	49
1:2048	24
Mock	0

Every 4 days, the G418-containing medium was removed and replaced to maintain selective pressure. Since geneticin works best during cell division, passaging was

performed frequently at less than 50% confluency. After two weeks, the cell cultures were observed under a confocal microscope. At the highest G418-concentrations, all cells were dead, and at the lowest concentrations, most cells were still alive. A well were only a few surviving cells could be found was chosen, since these cells could be assumed to carry the plasmid with geneticin resistance. These cells were transferred to a fresh 12-well plate with a lower geneticin concentration of $1.5\,\mathrm{mg\,ml^{-1}}$ and had been diluted to a concentration of one cell per well, to obtain clonal colonies. After the cells had reached 70% confluency they were passaged. The culture in each well was split, and transferred to wells on two separate 12-well plates so that one daughter culture could be fixed for imaging and the other culture could be kept alive. The cells were then stained with a streptavidin-conjugated fluorophore to confirm that they carried *Vamp2-Sbp* along with the geneticin resistance. A culture which carried the insert and did not show an abnormal phenotype was selected for future co-culturing.

3.10 Cell fixing, mounting and staining

The method used in this section is described in "Chemical and physical fixation of cells and tissues: an overview" by BQ Huang and EC Yeung [47].

Cells were fixed for 10 minutes at room temperature with freshly prepared electron microscopy grade 4% formaldehyde in Dulbecco's phosphate buffered saline^{++} (DPBS^{++}) (with Ca^{++} and Mg^{++}) from Gibco Catalog #: 14040133). The cells were then washed three times for five minutes, with DPBS^{++}, and then incubated for 30 minutes at room temperature with a 1:200 dilution, in DPBS^{++}, of each of the corresponding fluorescent compounds, excluding DAPI. The set of fluorophores used with each cell-type is listed in table 3.4. All fluorophores were bought from Thermo Scientific.

Table 3.4: Fluorophore combinations used for each cell-treatment

	Egfp-Myo10	*Vamp2-Sbp*	*Gfp-Cfl1*
Nuclei	DAPI	DAPI	DAPI
Actin-filaments	Phalloidin-568	Phalloidin-488	Phalloidin-568
Protein of interest	N/A	Streptavidin-570	N/A

After incubation with the fluorophores, the cells were quickly washed with DPBS^{++} for 5 minutes at room temperature, after which a 1:10000 dilution of DAPI in DPBS^{++} was added and incubated for 3 minutes at room temperature. After this stage, the cells were kept in darkness under aluminum foil. The cells were washed 3 times with DPBS^{++} for 5 minutes each time, after which they were immediately mounted. ProLong Diamond Antifade mounting medium from Thermo Scientific (Catalog #: P36962) was added onto clean glass slides. Glass coverslips with the fixed and stained cells were washed with distilled water and attached to the slides by capillary force. The slides were then dried at room temperature overnight, with precaution taken to keep them in darkness at all time. The following day, the edge of the coverslips were sealed with nail polish, and then stored at 4 °C until imaged.

4

Results and discussion

4.1 mRNA transfections produce low yield, unspecific expression, and indications of cytotoxicity in NIH3T3 cells

The first step of the thesis project (see figure 1.1 for a schematic of the project plan) was to generate two cell types: FECs that expressed filopodia, and NECs that carried a membrane tag for separation at a later stage. To induce filopodia-formation in the FECs, NIH3T3 cells were to be transfected with *Egfp-Myo10*. There are many different methods available to introduce DNA and mRNA into mammalian cells, but the efficiency and toxicity of these methods may vary between cell types [48]. For this reason, both mRNA- and DNA transfection using different reagents was to be tried. In the initial attempts to generate FECs, NIH3T3 cells were transfected with *Egfp-Myo10* mRNA using the Lipofectamine MessengerMAX reagent.

The results, which are presented in figure 4.1, seemed promising at first, since a strong fluorescence signal was detected when exciting the sample with the 488 nm channel. This implied expression of *Egfp-Myo10* in the cells, which in turn implied successful transfection. However, due to the distribution of the signal, concerns were soon raised. There are two main clues that the source of the signal is not EGFP-MYO10. The first clue is signal emission from every cell in the sample, which suggests a perfect uptake and expression of the mRNA. While virus-mediated DNA delivery methods may achieve transfection efficiency rates of close to 100%, cationic lipid-based transfection reagents such as the ones used in this project are generally much less effective in this regard [49]. The second clue that the signal was a false positive is the location of the source within the cells. If the source is EGFP-MYO10 it would co-localize with the actin cytoskeleton, aggregated along the filaments that stretch between the adhesion points where the cells attach to the substrate. These signals however, mainly originated from within the main body of the cells. Rather than the cytoskeleton, the fluorescence signal appears to come from the mitochondrial network, resembling squiggly lines that surround the nuclei [50].

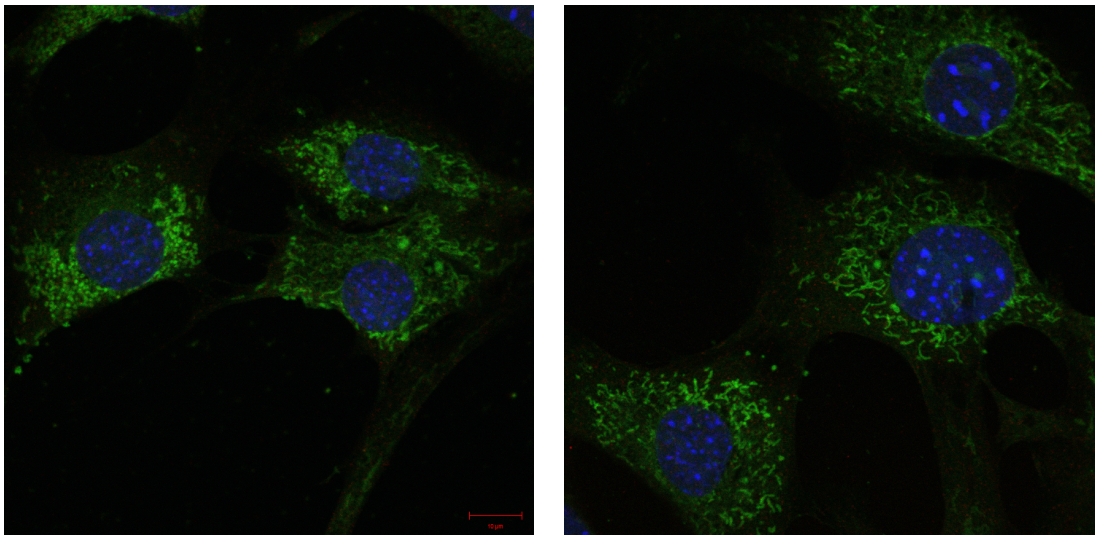

(a) **(b)**

Figure 4.1: Cells cultured on poly-D-lysine coated coverslips, transfected with *Egfp-Myo10* mRNA using the Lipofectamine MessengerMAX transfection reagent. (a) Cells fixed and stained 16 hours post transfection. (b) Cells fixed and stained 24 hours post transfection. In both images, the nuclei were stained with DAPI (shows as blue), and actin was stained with Phalloidin-570 (shows as red). The green on the images are excitations in the 488 nm channel. The images were taken with a Zeiss LSM700 inverted confocal microscope.

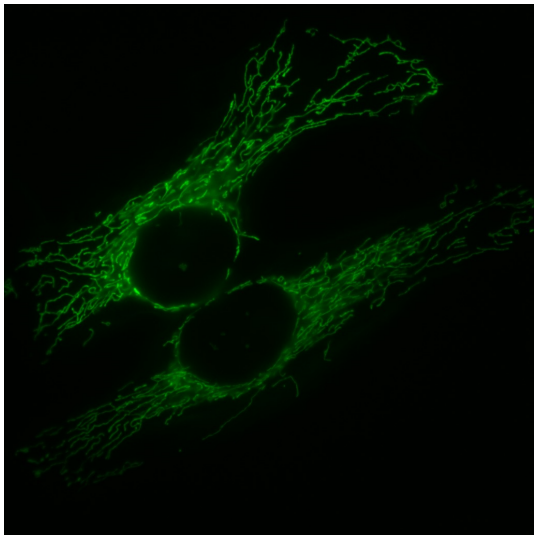

Figure 4.2: Image of the mitochondrial network in healthy HeLa cells expressing a mitochondrially targeted version of GFP (mtGFP). Reprinted under the Creative Commons Attribution 4.0 International license, `https://creativecommons.org/licenses/by/4.0/`. The original image is taken by Simon Troeder and can be found at `https://commons.wikimedia.org/wiki/File:HeLa_mtGFP.tif#/media/File:HeLa_mtGFP.tif` [51]

Mitochondrial autofluorescence is a known indicator of cytotoxicity in the form of oxidative stress. There are further symptoms of cellular malfunction to be found in the morphology of the mitochondria. Healthy mitochondrial networks are strictly tubular in their appearance. When subjected to oxidative stress, the network begins to break up into vesicular fragments [52]. Such dot-like fragments are visible mainly in the leftmost cell in figure 4.1. An example of a healthy mitochondrial network is included in figure 4.2 for comparison.

To introduce their payload DNA or mRNA, transfection reagents need to bypass the cells' phospholipid membranes. It is known that the complexes that are formed by cationic lipid reagents and their DNA- or RNA payload adhere to the membranes electrostatically before entering the cell by endocytosis, although much of the mechanism and intracellular fate of the complexes remains debated [49]. In the case of mRNA-transfection, only the outermost cellular membrane needs to be penetrated to enable translation by cytoplasmic ribosomes, and in the case of DNA-transfection, yet another membrane - namely the nuclear envelope - must be bypassed. By the nature of their purpose, cationic lipid-based transfection reagents can therefore interact with several cellular phospholipid bilayers by one means or another. The inherent risk in using such reagents is that it the cytoplasm and nucleus are not the only cell structures that rely on membranes to function. Mitochondria, for example, use phospholipid bilayers as the medium for the electron transport chain, which enables cellular respiration through the citric acid cycle [53]. If the mitochondrial membranes are compromised, this may cause the generation of free radicals and reactive oxygen species that in turn cause oxidative stress and the aforementioned autofluorescence. Transfection reagents that are toxic to some cell types may be mild to others, so successful transfection relies on finding a combination of cell type and reagent that works [54, 48]. Compatibility can be difficult to predict, and the fastest approach may simply be trial and error.

Egfp-Myo10 was not the only fusion gene used for mRNA-transfection in these initial attempts. In figure 4.3 is presented a fluorescence microscopy image from transfections using *Vamp2-Sbp*. As the streptavidin-conjugated fluorophore used is excited with a different wavelength than the autofluorescence from the mitochondria - and therefore is imaged in a different channel on the microscope - this image allows a better estimate of the transfection efficiency. As seen in the image, the fraction of *Vamp2-Sbp* expressing cells is low. This would pose a problem when co-culturing the NECs and FECs, since the NECs would be so dispersed that only a small fraction of the separable cells could be expected to be touched by filopodia from the FECs. By extension, this could mean that any transcriptional response that the filopodial contact induced in those cells may be indistinguishable from random noise. Despite the availability of samples of other lipid-based mRNA-transfection reagents that could be tried, mRNA transfection had some inherent disincentives to consider when deciding on the next step; mRNA is an unstable molecule even in very cold storage, which implied that fresh mRNA would have to be synthesized continuously. Furthermore, the pcDNA3.1(+)-VAMP2-SBP plasmid lacked the SP6 promoter and Kozac sequence required for mRNA translation in the cells. Before synthesizing the *Vamp2-Sbp* mRNA used in this experiment, those essential sequences had been introduced before the fusion gene on an overhanging PCR primer. There was still

a considerable amount of this PCR amplicon left, but in the possible event of a depletion, this too would add a step to the production process. Over the course of the six months I was to join the project, the workload of mRNA synthesis was likely to add up to a sizeable amount of man-hours. For these reasons, it was decided to switch the focus to transfection using whole plasmids.

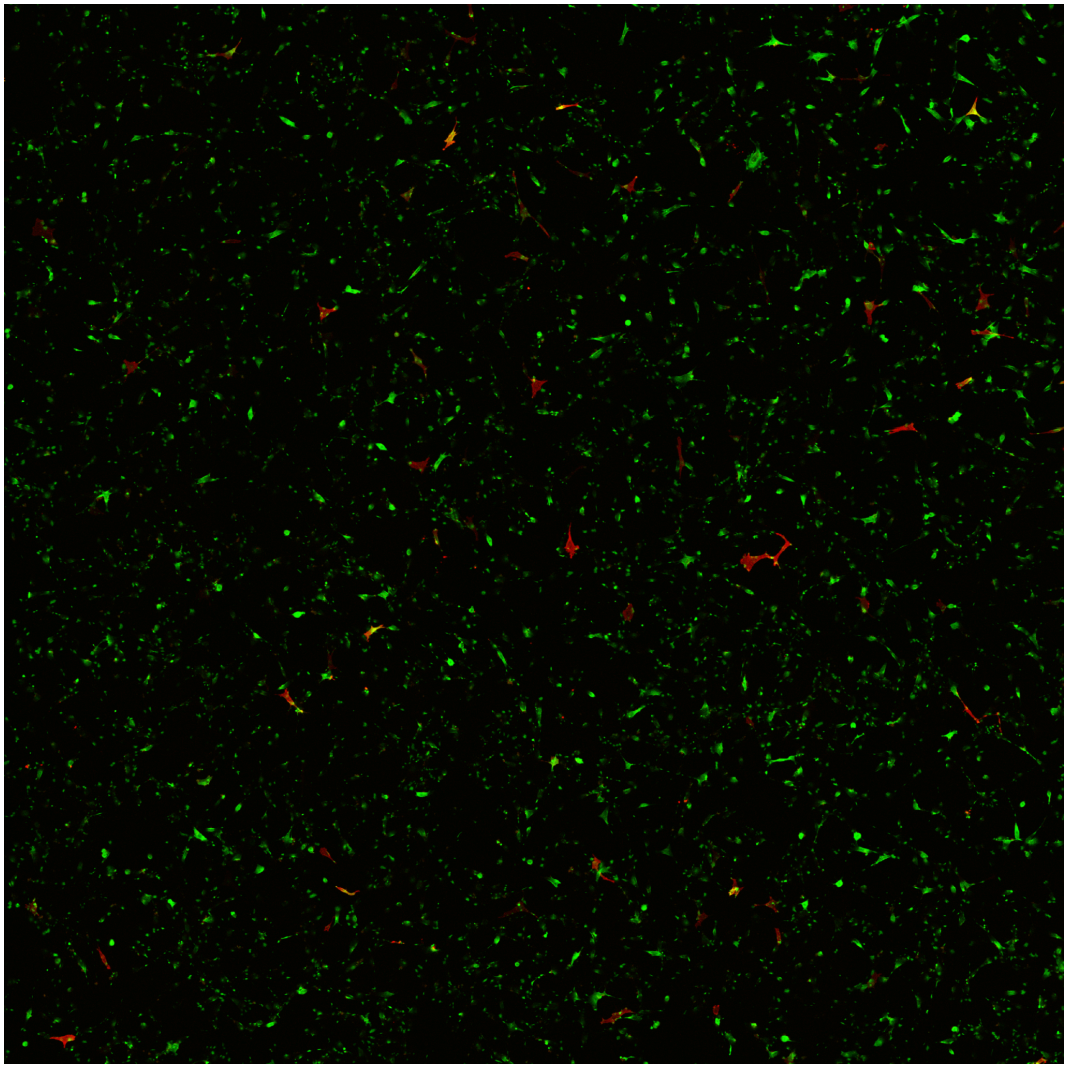

Figure 4.3: Cells cultured on poly-D-lysine coated coverslips, transfected with *Vamp2-Sbp* mRNA using the Lipofectamine MessengerMAX transfection reagent. Cells were fixed and stained 24 hours post transfection. Nuclei were stained with DAPI (shows as blue), actin was stained with Phalloidin 488, and VAMP2-SBP was stained with streptavidin-568.

4.2 Poly-D-lysine coating of coverslips may not permit filopodia-formation

After deciding against mRNA transfection, those initial experiments were recreated using whole plasmid transfection with the Lipofectamine LTX - PLUS reagent. Figure 4.4 shows mock cells, that were treated with the transfection reagent as if they were transfected, but without any plasmid payload. The image shows no indication of cytotoxicity in either phenotype or degree of confluency. Figure 4.5 shows cells that were transfected with *Egfp-Myo10* plasmids. Some cells are EGFP-expressing, confirming successful transfection. Although the cells display a healthy phenotype, there is no apparent difference in phenotype between *Egfp-Myo10* overexpressing cells and cells that do not express the fusion gene. The phenotype also seems identical to that of the mock cells in figure 4.4.

Myo10 is known to have induced filopodia formation in NIH3T3-cells using the transfection reagent Lipofectamine 2000 [44], which is another lipoplex-forming reagent from the same manufacturer as Lipofectamine LTX - PLUS. These results led to the hypothesis that the poly-D-lysine coating did not allow filopodia to form. Poly-D-lysine allows cell attachment by pure electrostatic interaction between the cells and the culture surface [55]. Filopodia are believed to rely on the formation of integrin adhesion points along the filopodia, and integrins bind to ECM-components such as fibronectin and laminin. While fibroblasts are ECM-producers and may secrete some ECM-components of their own, it is possible that those components were not present in concentrations high enough to permit filopodia-formation, or that fibroblasts do not produce ECM under the conditions of this experiment. For that reason, it was decided to attempt coating the coverslips with Geltrex Reduced Growth Factor Basement Membrane Matrix, which contains ECM-components.

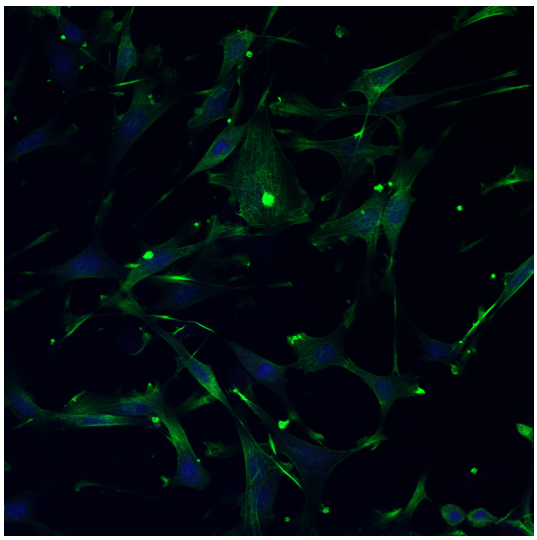

Figure 4.4: Mock-cells cultured on poly-D-lysine coated coverslips, transfected with a blank sample using the Lipofectamine LTX - PLUS transfection reagent. Cells were fixed and stained 24 hours post transfection. Nuclei were stained with DAPI (shows as blue), and actin (shown as green) was stained with Phalloidin 570.

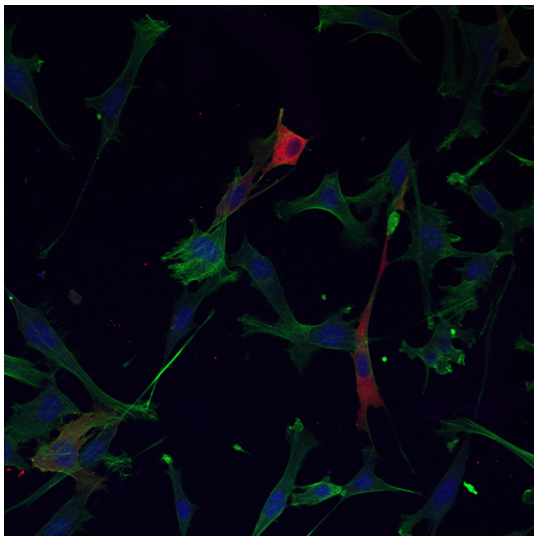

Figure 4.5: Cells cultured on poly-D-lysine coated coverslips, transfected with pCS2-EGFP-MYOX using the Lipofectamine LTX - PLUS transfection reagent. Cells were fixed and stained 24 hours post transfection. Nuclei were stained with DAPI (shows as blue), actin (shown as green) was stained with Phalloidin 570, and EGFP (shown as red) is excited in the 488 nm channel.

4.3 Formation of filopodia-like protrusions can be induced with cofilin on Geltrex-coated coverslips.

After considering that polylysinated coverslips may lack actin-anchoring sites necessary for filopodia-formation, cells were transfected using *Egfp-Myo10* plasmids on coverslips coated with Geltrex Reduced Growth Factor Basement Membrane Matrix. The results are imaged in figure 4.6. These attempts did not generate filopodia-forming cells, and resulted in a transfection rate and phenotype seemingly identical to the *Myo10*-transfections on polylysinated coverslips. As stated before, transfection using plasmids containing a *Gfp-Myo10* fusion gene has been used to successfully induce filopodia-formation in experiments by Tokuo *et al.* [44] under conditions that were only slightly different from the setup used in this thesis. Tokuo *et al.* used an American NIH3T3-strain seeded on pure fibronectin, and the cells were transfected with a customized *Gfp-Myo10* plasmid using the Lipofectamine 2000 reagent. The cells in figure 4.6 are a Swiss NIH3T3-strain grown on a purified basement membrane matrix. It is noteworthy that fibronectin is not a basement membrane-component [56], which prompts the question whether fibronectin-binding is necessary for *Myo10*-induced filopodia formation in NIH3T3-cells.

In generating the NECs, filopodia-formation was to be inhibited. This was to make sure that the NEC transcriptional profile was to be generated only from non filopodia-forming cells. Initially, the intention was to apply the method used by Fierro-Gonzaléz *et al.* and inhibit filopodia using DECMA-1 anti-E-cadherin antibodies. Figure 4.8 shows images from such an experiment, where cells were treated

with a range of increasing antibody concentrations. In these images, there is no visible change from a normal fibroblast phenotype between the different treatments. There are no filopodia visible in either the treated cells or in the control cells. Since the control cells did not form filopodia, it is impossible to tell whether the antibodies had the intended effect. As seen in our other experiments, these cells do not form filopodia on polylysinated coverslips, neither spontaneously nor when transfected with *Myo10*. However, before antibody-inhibition was attempted in combination with another coverslip-treatment, the idea was of using antibodies for this purpose was abandoned. Antibodies could possibly "bleed" in a NEC/FEC co-culture and cause unwanted inhibition of filopodia in the FECs. Therefore, a different approach was investigated where the NECs were transfected with a filopodia-inhibiting gene. The use of cofilin to inhibit filopodia has been described by Breitsprecher *et al.* [57]. Figure 4.7 shows cells transfected with *Gfp-Cfl1* on Geltrex-coated coverslips. This experiment generated results opposite to expectation, inducing filopodia-formation in every cell that successfully expressed *Gfp-Cfl1*. As seen in the figure, GFP-cofilin aggregated in long actin-rich protrusions. At high cofilin concentrations, actin filaments may be partially severed into shorter segments that bundle together to form long rod-like aggregates. This raises the question whether the protrusions in figure 4.7 are actually true filopodia, or rather "rods" of aggregated short actin filaments that become so long that they cause the protrusions. However, rods cannot be stained with phalloidin [58]. Since phalloidin co-localized with the protrusions in our experiment, it is likely that cofilin-overexpression actually induced filopodia-formation. Cofilin is known to stimulate polymerization or depolymerization of F-actin depending on parameters such as cofilin concentration, or the concentration of other actin-binding proteins [59, 21]. Suggesting that the protein has the ability to both inhibit or stimulate filopodia-formation. After I left this project, these experiments have been repeated, confirming that filopodia-formation can be induced by cofilin-overexpression. This provides a reliable way to generate FECs from NIH3T3-cells, which is essential for the future success of the project. This still leaves us without a method for inhibiting filopodia in the NECs, but since filopodia do not seem to form spontaneously in these cells under the given conditions, that may not be necessary.

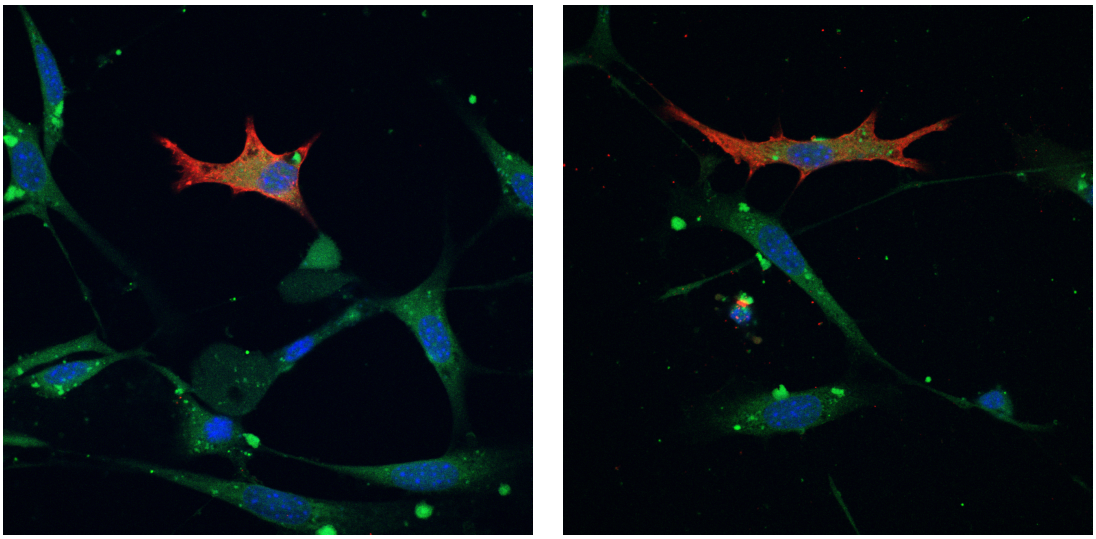

(a)

(b)

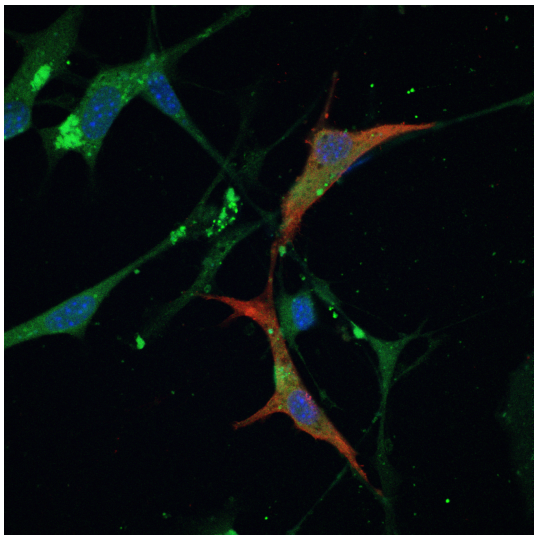

(c)

Figure 4.6: Cells cultured on Geltrex-coated coverslips, transfected with pCS2-EGFP-MYOX using the Lipofectamine LTX- PLUS transfection reagent. (a) Cells fixed and stained 24 hours post transfection. (b) Cells fixed and stained 24 hours post transfection. In both images, the nuclei were stained with DAPI (shows as blue), and actin was stained with Phalloidin-570 (shows as green), and EGFP (shown as red) is excited in the 488 nm channel.

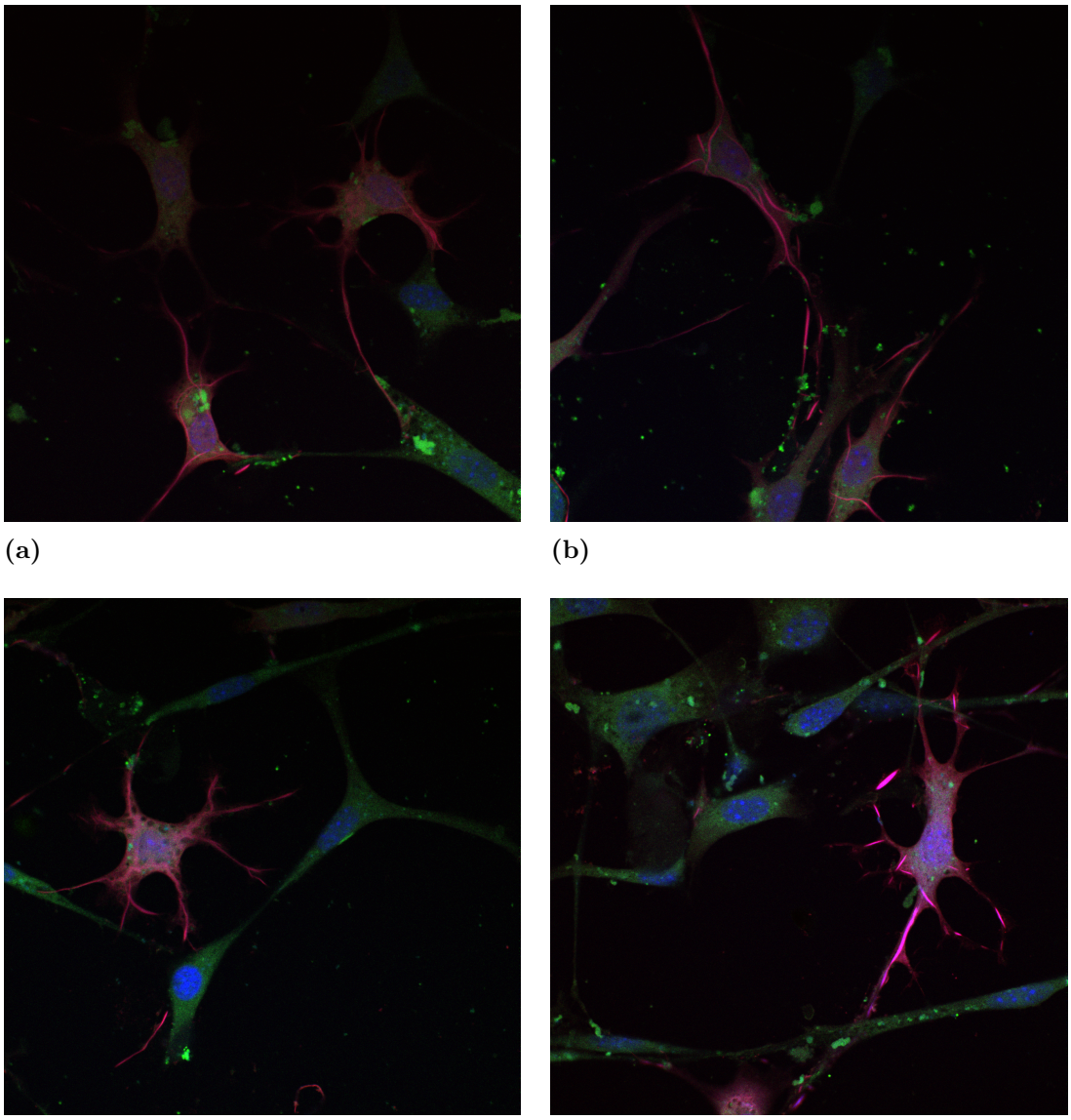

(a) **(b)**

(c) **(d)**

Figure 4.7: Cells cultured on Geltrex-coated coverslips, transfected with pCS2-GFP-Cofilin using the Lipofectamine LTX - PLUS transfection reagent. (a) Cells fixed and stained 16 hours post transfection. (b) Cells fixed and stained 24 hours post transfection. In both images, the nuclei were stained with DAPI (shows as blue), and actin was stained with Phalloidin-570 (shows as green) and GFP (shown as red) is excited in the 488 nm channel.

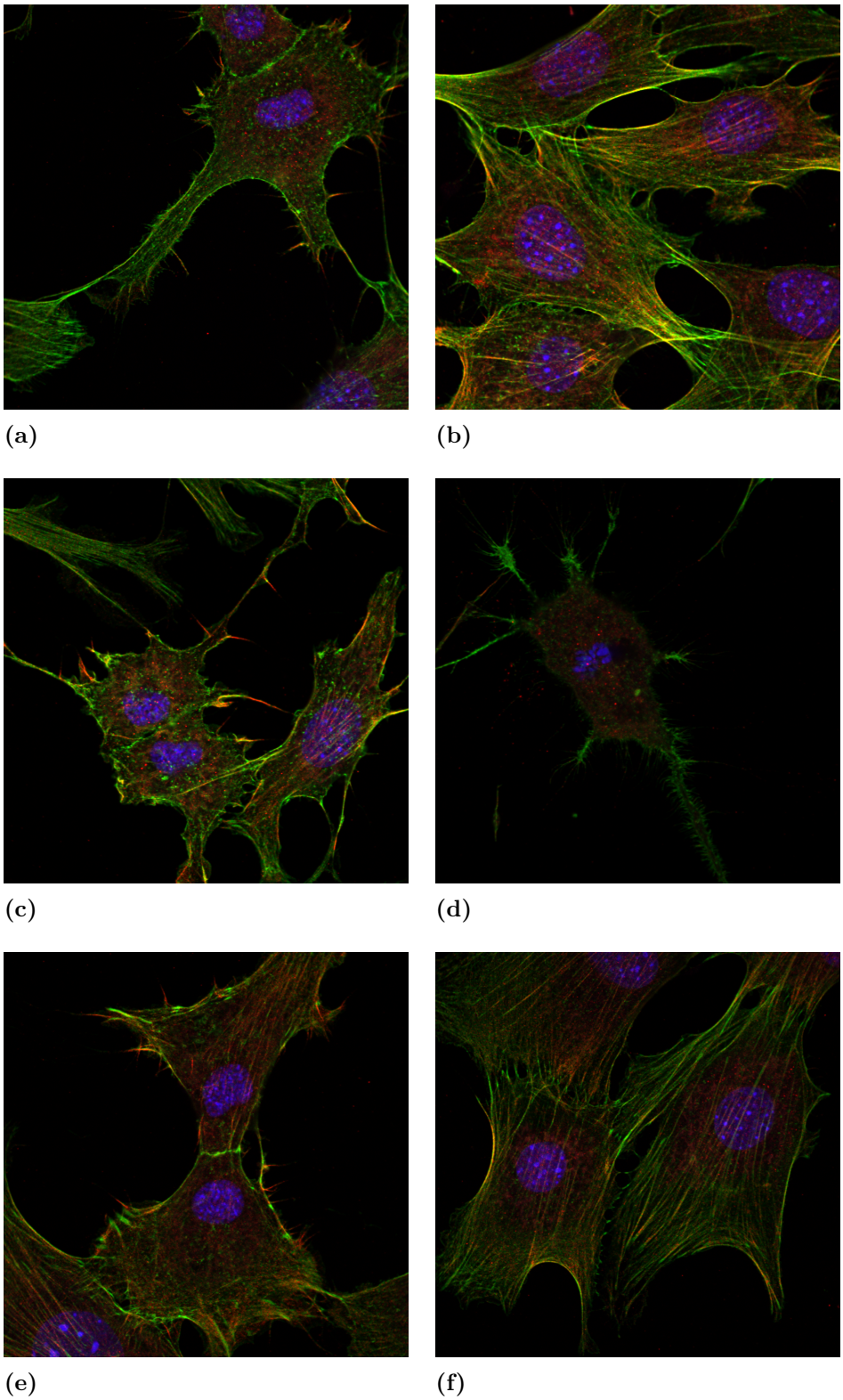

Figure 4.8: Images of filopodia inhibition using DECMA-1 antibodies in varying dilutions. The nuclei were stained with DAPI (shows as blue), anti-MYO10 (shows as red), and actin was stained with Phalloidin-570 (shows as green). The fractional content of DECMA-1 antibodies is as follows: (a) 1:600 (b)1:800 (c) 1:1200 (d) 1:2400 (e), (f) Mock inhibitions without antibodies.

4.4 Low transfection efficiency of *Vamp2-Sbp* motivated the generation of a stable cell line.

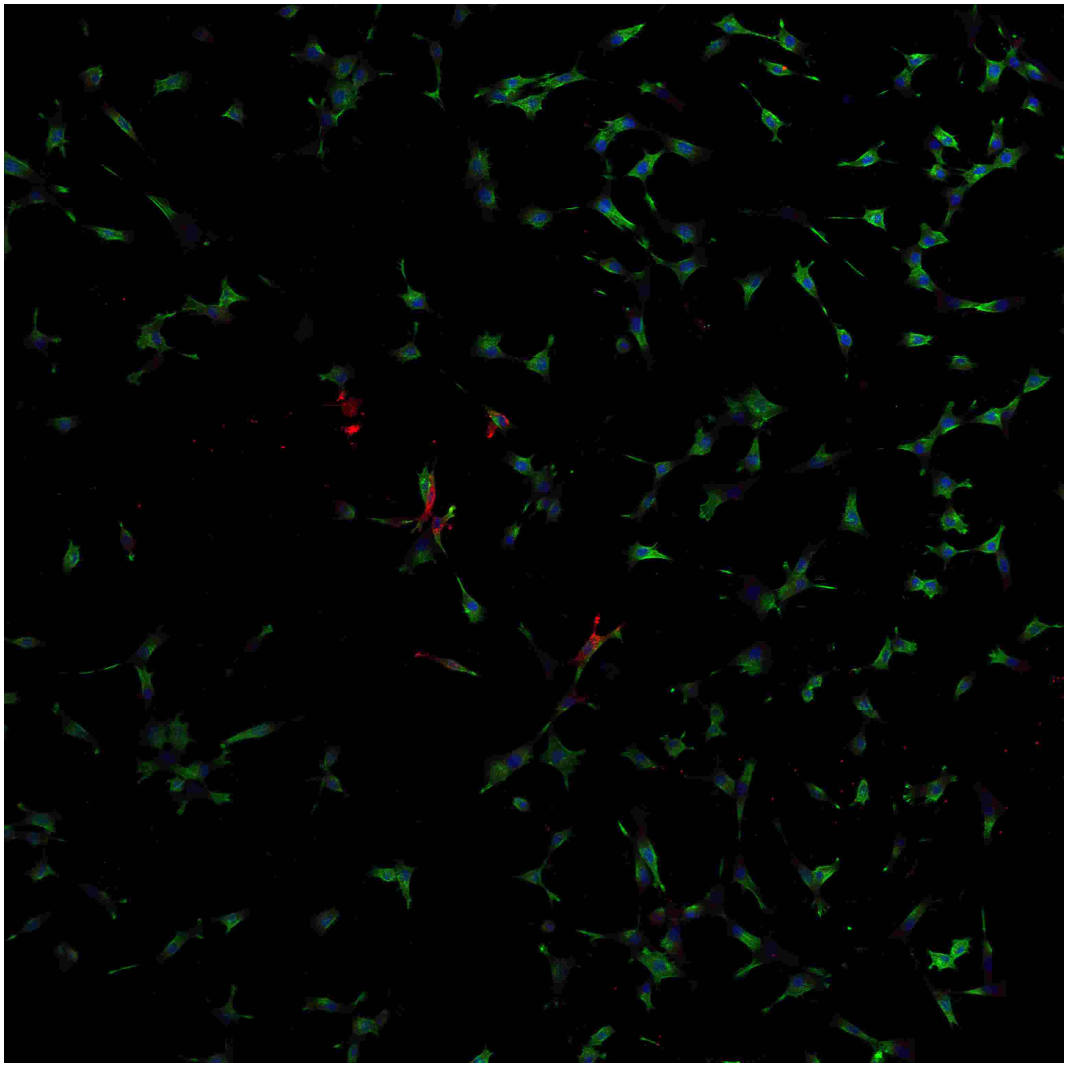

Figure 4.9: Cells cultured on poly-D-lysine coated coverslips, transfected with pcDNA3.1(+)-VAMP2-SBP using the Lipofectamine LTX - PLUS transfection reagent. Cells were fixed and stained 24 hours post transfection. Nuclei were stained with DAPI (shows as blue), actin (shown as green) was stained with Phalloidin 488, and VAMP2-SBP was stained with streptavidin-568 (shown as red).

The *Vamp2-Sbp*-plasmid transfected cells shown in figure 4.9 are comparable to the *Myo10*-transfections shown in figure 4.5, with a healthy phenotype, but a low transfection rate. As mentioned in section 4.1, a low transfection efficiency for the *Vamp2-Sbp*-expressing NECs had troubling implications. Separation using streptavidin-conjugated magnetic beads after co-culturing and filopodial contact would only be possible for cells that expressed *Vamp2-Sbp*. If those cells were too far dispersed in the co-culture, the probability of a cell being both separable and also having been in filopodial contact with an FEC became lower. It seemed likely

that for each such cell, there would be many NECs that had not been touched by FECs, which in turn would make the transcriptional response for filopodial contact difficult to see. This problem was amplified by an equally low transfection efficiency in the FECs.

There was however a possible way to make a culture which consisted solely of *Vamp2-Sbp* expressing cells, namely the generation of a stable cell line. Expression from transfected plasmids is transient, due to plasmid degradation and a selective pressure for descendants of the transfected cells to lose the plasmids if they are not essential for the survival of the cells. A resistance gene against the G418 antibiotic incorporated on the pcDNA3.1(+)-VAMP2-SBP plasmid allowed for the generation of a cell line of *Vamp2-Sbp* expressing cells. Post transfection, cells were incubated in an antibiotic titration with varying concentrations of geneticin. Brightfield microscopy images of cell cultures that underwent the treatment are presented in figure 4.10. At high concentrations of the antibiotic, all cells - even those cells that had been successfully transfected with the resistance gene - were unable to survive, and at low concentrations even cells that lacked resistance were able to endure. To generate a cell line where all cells could be presumed to carry and express the plasmid, a culture was picked where only a few cells survived the antibiotic pressure. Image (b) in figure 4.10 shows the selected cell-culture. In this image, aggregates of dead cells dominate, but a few cells with a healthy fibroblast phenotype remained. These cells were reseeded in a lower geneticin concentration at a density of $\tilde{1}$ cell per well and proliferated. Samples from these cultures were imaged under a fluorescence microscope with a streptavidin-conjugated fluorophore to verify that the plasmids were intact and still contained *Vamp2-Sbp*, rather than just the geneticin resistance gene. Figure 4.11 shows fluorescence microscopy images of a selection of the generated stable cell lines. A cell line that did not contain aberrant cells, such as the enlarged cells in image (b) in the figure, was selected for further culturing.

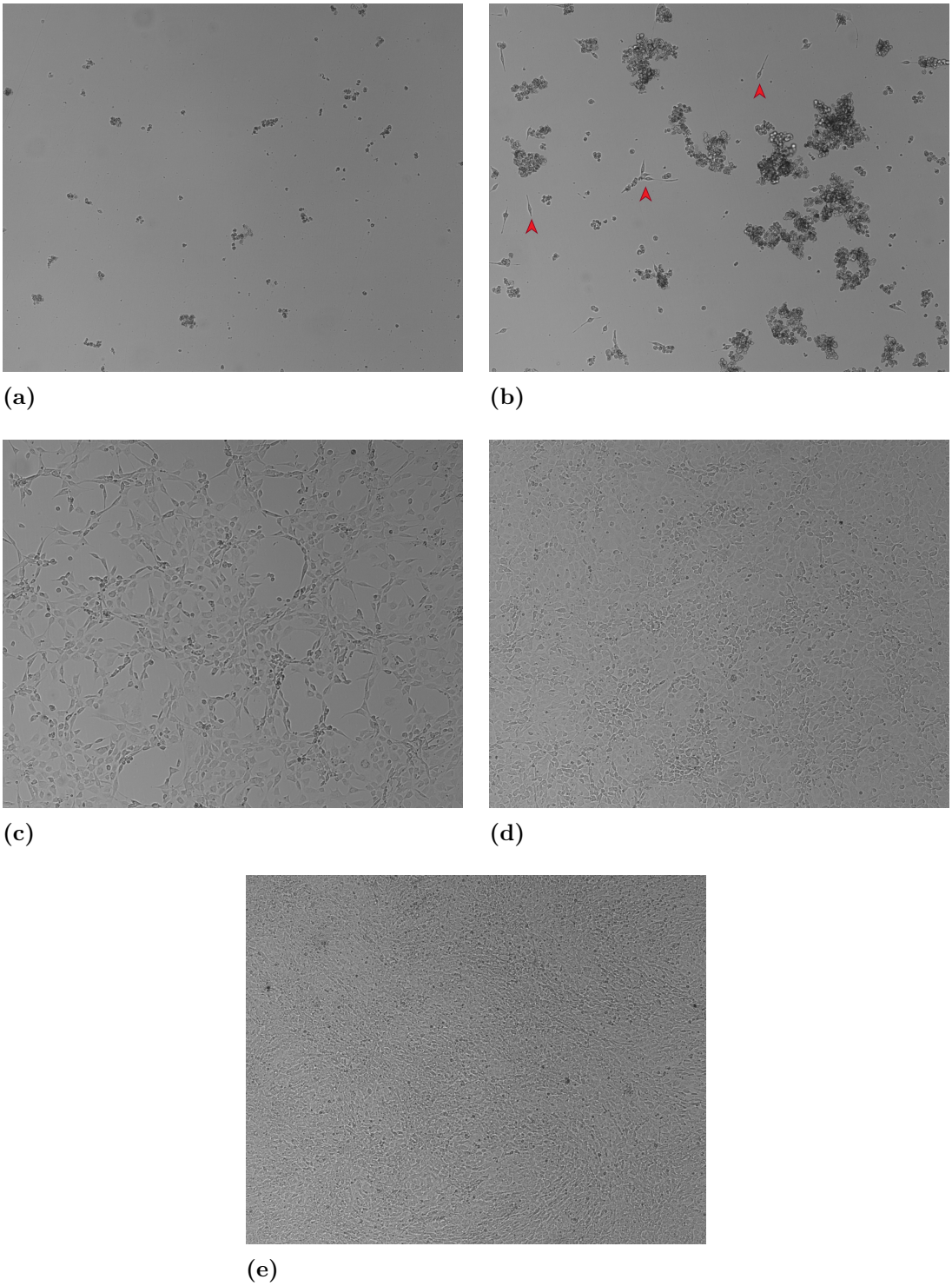

Figure 4.10: A representative selection of brightfield microscopy images of NIH3T3 murine embryonic fibroblasts after two weeks of culturing in geneticin-enriched medium of varying dilutions. The fractional content of geneticin in the images is as follows: (a) 1:32 (b) 1:64 (c) 1:256 (d) 1:512 (e) 1:1024. In image (b), the arrowheads indicate healthy cells. A full list of the dilution series, as well as the actual concentration of geneticin, can be found in table 3.3.

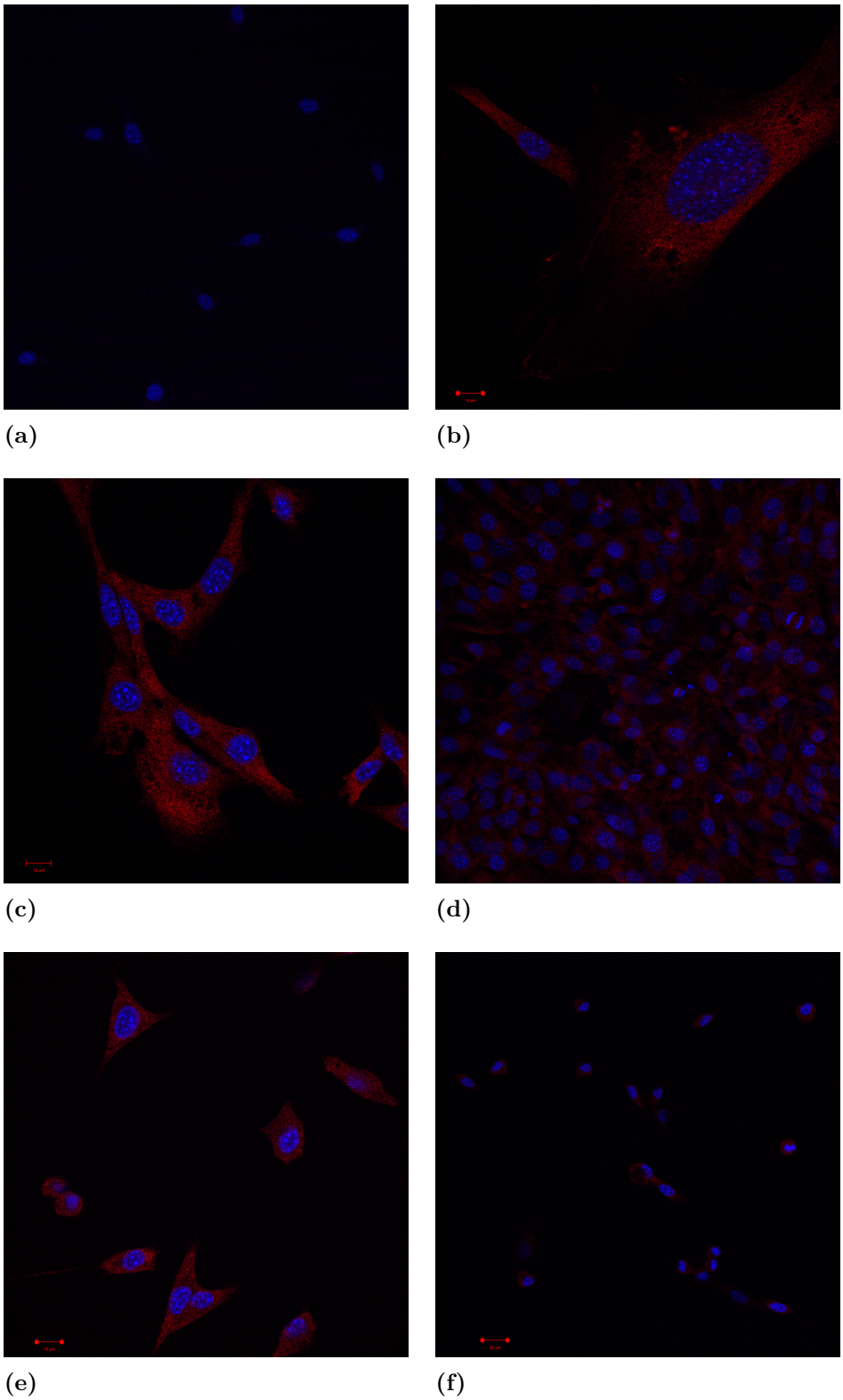

Figure 4.11: Selected representative images of the generated stable cell line. The nuclei were stained with DAPI (shows as blue), and VAMP2-SBP was stained with streptavidin-568 (shows as red). (a) Mock cells, cultured without the selective pressure of geneticin. (b) Example of *Vamp2-Sbp*-expressing cells showing geneticin-induced aberrations, here in the form of enlarged nucleus. (c), (d) One healthy culture, stably expressing *Vamp2-Sbp*. (e), (f) Another healthy culture, stably expressing *Vamp2-Sbp*.

5
Conclusion

The aim of this project was to better understand on the genetic level how filopodia help mediate compaction of the mammalian embryo. This was to be done using a model system consisting of a co-culture of murine embryonic fibroblasts consisting of roughly equal parts filopodia-expressing cells (FECs) and non-expressing cells (NECs), and then isolating the NECs to perform a gene-expression analysis of the transcriptional response to filopodial contact. Going into the project, it was understood by me and my supervisor that it was an ambitious undertaking, and that we were unlikely to finish it during the half year I would join the project. Figure 1.1 in the introduction of this thesis is a schematic overview of the project plan. At the time I left the project, we had reached and completed the first step of this outline, which is finding a method of inducing filopodia in the FECs, and generating NECs using a membrane marker.

Initial mRNA-transfections of the fibroblasts resulted in signs of toxicity, possibly because of compatibility problems between the cell type and the transfection reagent. Because of this, all subsequent transfections were performed using whole plasmids.

To generate the FECs, filopodia-formation was induced by transfecting fibroblasts with *Cfl1* (cofilin). The intended effect of transfecting cells with this gene was actually to inhibit filopodia formation in the NECs, as described by Breitsprecher *et al.* [57]. The following literature study revealed that cofilin may promote either polymerization or depolymerization of actin, depending on parameters such as cofilin concentration or the levels of other actin-binding proteins present in the cells.

Fierro-Gonzaléz *et al.* had induced filopodia-formation in mouse embryos by transfection with *Myo10* [1]. Transfecting embryonic fibroblasts with *Myo10* did not generate filopodia in our experiments. Initial attempts to do so may have failed due to the polylysine coating of coverslips, which lack ECM-components necessary for integrin adhesion. Switching to a coat consisting of basement membrane matrix did not allow filopodia-formation when transfecting with *Myo10*. It is not clear why this approach did not work, but it is possible that *Myo10*-transfection of NIH3T3-cells cannot induce filopodia unless the cells are seeded on fibronectin, which is not present in basement membranes. Tokuo *et al.* used *Myo10* to generate filopodia in NIH3T3-cells seeded on pure fibronectin [44].

To equip NECs with a membrane marker that allows separation using streptavidin-conjugated magnets, embryonic fibroblasts were transfected with *Vamp2-Sbp*. To solve the issue of low transfection efficiency, antibiotic resistance on the *Vamp2-Sbp* plasmid was used to successfully generate a stable cell line, consisting entirely of cells expressing the marker. At the time of writing, supervisor Emanuele Celauro has suc-

cessfully separated NECs from a co-culture with control cells using the VAMP2-SBP marker on a MACS column. Thus, significant headway has been made towards co-culturing the FECs and NECs, separating the populations, and then performing a gene-expression analysis of the NECs.

Bibliography

[1] Fierro-González JC, White MD, Silva JC, Plachta N. Cadherin-dependent filopodia control preimplantation embryo compaction. Nature Cell Biology;(12):1424–1433.

[2] Mattila PK, Lappalainen P. Filopodia : molecular architecture and cellular functions. 2008;9(June).

[3] Maître JL, Niwayama R, Turlier H, Nédélec F, Hiiragi T. Pulsatile cell-autonomous contractility drives compaction in the mouse embryo. Nature Cell Biology. 2015;17(7):849–855. Available from: `http://www.nature.com.sire.ub.edu/ncb/journal/v17/n7/full/ncb3185.html`.

[4] Gallicano GI. EMBRYOS. 2001;p. 1089–1108.

[5] Salas-vidal E, Lomelı H. Imaging filopodia dynamics in the mouse blastocyst. 2004;265:75–89.

[6] Morris SA, Teo RTY, Li H, Robson P, Glover DM. Origin and formation of the fi rst two distinct cell types of the inner cell mass in the mouse embryo. 2010;107(14).

[7] Rossant J, Tam PPL. Blastocyst lineage formation, early embryonic asymmetries and axis patterning in the mouse. Development (Cambridge, England). 2009;136(5):701–13. Available from: `http://www.ncbi.nlm.nih.gov/pubmed/19201946`.

[8] Stephenson RO, Yamanaka Y, Rossant J. Disorganized epithelial polarity and excess trophectoderm cell fate in preimplantation embryos lacking E-cadherin. Development. 2010;137(20):3383–3391.

[9] Oliveira MS, Barreto-Filho JB. Name of journal: World Journal of Stem Cells ESPS Manuscript NO: 14571 Columns: Minireviews Placental-derived stem cells: Culture, differentiation and challenges;.

[10] Chawengsaksophak K, de Graaff W, Rossant J, Deschamps J, Beck F. Cdx2 is essential for axial elongation in mouse development. Proceedings of the National Academy of Sciences of the United States of America. 2004;101(20):7641–7645.

[11] Brevini TAL, Pennarossa G. 2.2. In: Gametogenesis, Early Embryo Development and Stem Cell Derivation. New York: Springer; 2013. p. 32–35.

[12] Wood W, Martin P. Structures in focus — filopodia. The International Journal of Biochemistry and Cell Biology. 2002;34:726–730.

[13] Arjonen A, Kaukonen R, Ivaska J. Filopodia and adhesion in cancer cell motility. Cell Adhesion and Migration. 2011;5(5):421–430.

[14] Marjoram R, Guilluy C, Burridge K. Using magnets and magnetic beads to dissect signaling pathways activated by mechanical tension applied to cells. Methods. 2016;94:19–26.

[15] Sanders TA, Llagostera E, Barna M. Specialized filopodia direct long-range transport of SHH during vertebrate tissue patterning. Nature. 2013;497(7451):628–632.

[16] Malumbres M, Barbacid M. Mammalian cyclin-dependent kinases. Trends in biochemical sciences. 2005;30(11):630–641.

[17] UniProt. UniProt Knowledge Base Reports, Myosin X; 2017.

[18] Institute RP. RPI Biochemistry of Metabolism: Cell Biology, Myosin X; 2017.

[19] Berg JS, Cheney RE. Myosin-X is an unconventional myosin that undergoes intrafilopodial motility. Nature cell biology. 2002;4(3):246–250.

[20] UniProt. UniProt Knowledge Base Reports, Cofilin; 2017. Available from: `http://www.uniprot.org/uniprot/P23528`.

[21] Bamburg JR, Bernstein BW. Roles of ADF/cofilin in actin polymerization and beyond. F1000 Biol Rep. 2010;2(62.10):3410.

[22] Suzuki ST, Hirano S. Cadherin Superfamily. Springer; 2016.

[23] Kozma R, Ahmed S, Best A, Lim L. The Ras-related protein Cdc42Hs and bradykinin promote formation of peripheral actin microspikes and filopodia in Swiss 3T3 fibroblasts. Molecular and cellular biology. 1995;15(4):1942–1952.

[24] Kovářová M, Tolar P, Arudchandran R, Dráberová L, Rivera J, Dráber P. Structure-function analysis of Lyn kinase association with lipid rafts and initiation of early signaling events after Fc receptor I aggregation. Molecular and Cellular Biology. 2001;21(24):8318–8328.

[25] Nolan T, Hands RE, Bustin SA. Quantification of mRNA using real-time RT-PCR. Nature protocols. 2006;1(3):1559–1582.

[26] NCBI. NCBI Gene Reports, Oct4; 2017. Available from: `https://www.ncbi.nlm.nih.gov/gene/71950`.

[27] NCBI. NCBI Gene Reports, Sox2; 2017. Available from: `https://www.ncbi.nlm.nih.gov/gene/20674`.

[28] NCBI. NCBI Gene Reports, Nanog; 2017. Available from: `https://www.ncbi.nlm.nih.gov/gene/71950`.

[29] NCBI. NCBI Gene Reports, Eomes; 2017. Available from: `https://www.ncbi.nlm.nih.gov/gene/13813`.

[30] Yang C, Czech L, Gerboth S, Kojima Si, Scita G, Svitkina T. Novel roles of formin mDia2 in lamellipodia and filopodia formation in motile cells. PLoS biol. 2007;5(11):e317.

[31] Gustafson T, Wolpert L. On the Cellular Basis of Morphogenesis in the Sea Urchin Embryo. Experimental Cell Research. 1961;(22):437–449.

[32] Faix J, Rottner K. The making of filopodia;.

[33] Jacquemet G, Hamidi H, Ivaska J. Filopodia in cell adhesion, 3D migration and cancer cell invasion. Current opinion in cell biology. 2015;36:23–31.

[34] Adams CL, Chen YT, Smith SJ, Nelson WJ. Mechanisms of epithelial cell–cell adhesion and cell compaction revealed by high-resolution tracking of E-cadherin–green fluorescent protein. The Journal of cell biology. 1998;142(4):1105–1119.

[35] Turlier H, Maître Jl. Seminars in Cell & Developmental Biology Mechanics of tissue compaction. 2015;48:110–117.

[36] Ogle BM, Mooradian DL. The role of vascular smooth muscle cell integrins in the compaction and mechanical strengthening of a tissue-engineered blood vessel. Tissue engineering. 1999;5(4):387–402.

[37] Cui Xs, Li Xy, Shen Xh, Bae Yj. Transcription Profile in Mouse Four-Cell , Morula , and Blastocyst : Genes Implicated in Compaction and Blastocoel Formation. 2007;143(December 2005):133–143.

[38] Hirate Y, Hirahara S, Inoue Ki, Kiyonari H, Niwa H, Sasaki H. Par-aPKC-dependent and-independent mechanisms cooperatively control cell polarity, Hippo signaling, and cell positioning in 16-cell stage mouse embryos. Development, growth & differentiation. 2015;57(8):544–556.

[39] Samarage CR, White MD, Álvarez YD, Fierro-González JC, Henon Y, Jesudason EC, et al. Cortical tension allocates the first inner cells of the mammalian embryo. Developmental cell. 2015;34(4):435–447.

[40] Maître JL, Turlier H, Illukkumbura R, Eismann B, Niwayama R, Nédélec F, et al. Asymmetric division of contractile domains couples cell positioning and fate specification. Nature. 2016;536(7616):344–348.

[41] Maro B, Dard N, Louvet-valle S. Phosphorylation of ezrin on threonine T567 plays a crucial role during compaction in the mouse early embryo. 2004;271:87–97.

[42] NCBI. NCBI Gene Reports, VAMP2; 2017. Available from: `https://www.ncbi.nlm.nih.gov/gene/6844`.

[43] Keefe AD, Wilson DS, Seelig B, Szostak JW. One-step purification of recombinant proteins using a nanomolar-affinity streptavidin-binding peptide, the SBP-Tag. Protein expression and purification. 2001;23(3):440–446.

[44] Tokuo H, Mabuchi K, Ikebe M. The motor activity of myosin-X promotes actin fiber convergence at the cell periphery to initiate filopodia formation. J Cell Biol. 2007;179(2):229–238.

[45] Scientific T. Thermo Scientific Tm calculator; 2017. Available from: `https://www.thermofisher.com/se/en/home/brands/thermo-scientific/molecular-biology/molecular-biology-learning-center/molecular-biology-resource-library/thermo-scientific-web-tools/tm-calculator.html`.

[46] University N. Oligo Calc Oligonucleotide Properties Calculator; 2017. Available from: `http://biotools.nubic.northwestern.edu/OligoCalc.html`.

[47] Huang BQ, Yeung EC. Chemical and physical fixation of cells and tissues: an overview. In: Plant Microtechniques and Protocols. Springer; 2015. p. 23–43.

[48] Durán MC, Willenbrock S, Barchanski A, Müller JMV, Maiolini A, Soller JT, et al. Comparison of nanoparticle-mediated transfection methods for DNA expression plasmids: efficiency and cytotoxicity. Journal of nanobiotechnology. 2011;9(1):47.

[49] Bielke W, Erbacher C. Nucleic acid transfection. vol. 296. Springer Science & Business Media; 2010.

[50] Forkink M, Smeitink JA, Brock R, Willems PH, Koopman WJ. Detection and manipulation of mitochondrial reactive oxygen species in mammalian cells. Biochimica et Biophysica acta (BBa)-Bioenergetics. 2010;1797(6):1034–1044.

[51] University N. Oligo Calc Oligonucleotide Properties Calculator; 2017. Available from: https://commons.wikimedia.org/wiki/File:HeLa_mtGFP.tif#/media/File:HeLa_mtGFP.tif.
[52] Rodrigues RM, Macko P, Palosaari T, Whelan MP. Autofluorescence microscopy: a non-destructive tool to monitor mitochondrial toxicity. Toxicology letters. 2011;206(3):281–288.
[53] ;.
[54] Yamano S, Dai J, Moursi AM. Comparison of transfection efficiency of nonviral gene transfer reagents. Molecular biotechnology. 2010;46(3):287–300.
[55] Aldrich S. Poly-D-Lysine product description page; 2017. Available from: http://www.sigmaaldrich.com/technical-documents/articles/biofiles/poly-lysine.html.
[56] Kruegel J, Miosge N. Basement membrane components are key players in specialized extracellular matrices. Cellular and Molecular Life Sciences. 2010;67(17):2879–2895.
[57] Breitsprecher D, Koestler SA, Chizhov I, Nemethova M, Mueller J, Goode BL, et al. Cofilin cooperates with fascin to disassemble filopodial actin filaments. J Cell Sci. 2011;124(19):3305–3318.
[58] Bamburg JR, Bernstein BW. Actin dynamics and cofilin-actin rods in alzheimer disease. Cytoskeleton. 2016;.
[59] Umeki N, Hirose K, Uyeda TQ. Cofilin-induced cooperative conformational changes of actin subunits revealed using cofilin-actin fusion protein. Scientific reports. 2016;6.

A
Appendix: Plasmids

14/1/2017 18:57:42

pcDNA3.1(+)-VAMP2-SBP (5920 bp)

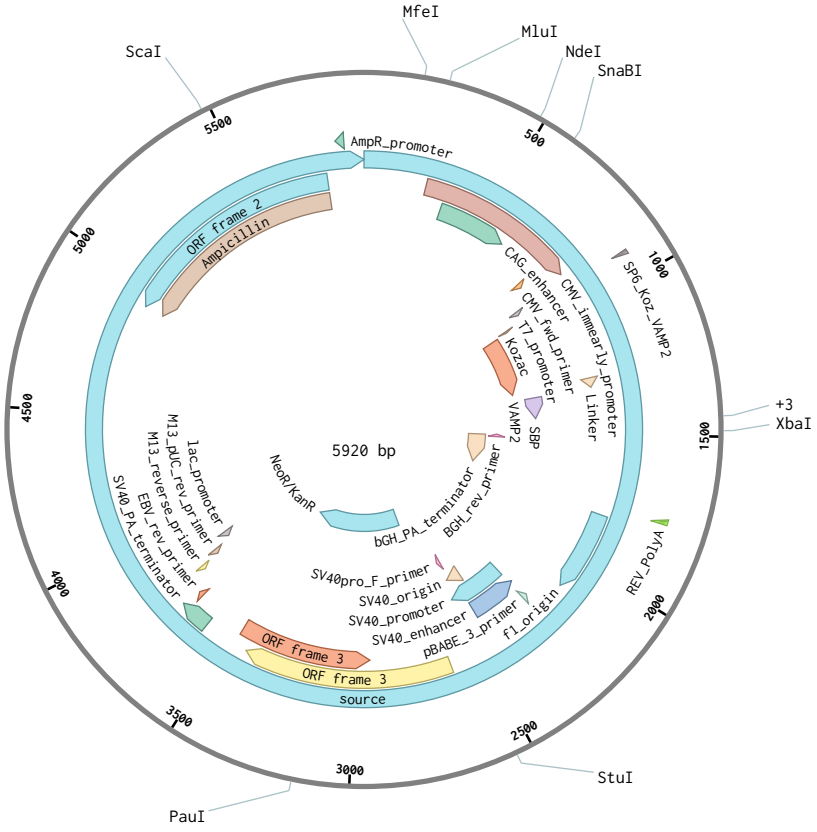

14/1/2017 18:57:09

pCS2-EGFP-MyoX (11361 bp)

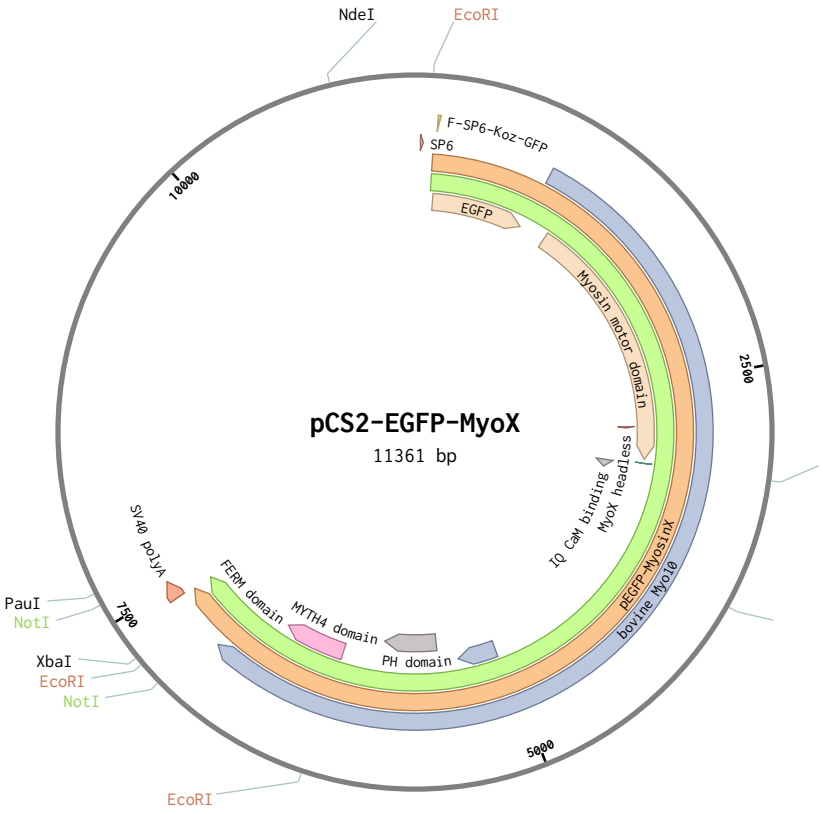

14/1/2017 18:56:14

pCS2 GFP-Cofilin (5441 bp)